The X_{17} Search at PADME: From Run III to Run IV upgrades

Marco Mancini on behalf of the PADME Collaboration

INFN - LNF, Università di Roma "Tor Vergata"

Frascati, X17 What if workshop - 19.03.2026

marco.mancini@lnf.infn.it

ATOMKI X_{17} anomaly – nuclear observation

Anomaly in the angular correlation of e^+e^- pairs emitted via IPC in the ^{8}Be, ^{4}He and ^{12}C nuclear de-excitation. It seems to be compatible with a **new neutral mediator called X_{17} :**

- $m_{X_{17}} \sim 17$ MeV
- $Br(e^+e^- \to X_{17}) \simeq 5\times10^{-6} Br(e^+e^- \to \gamma\gamma)$
- $\Gamma_{X_{17}} \simeq \frac{\epsilon^2 \alpha m_{X_{17}}}{3} \to \Gamma_V = 0.5 \left(\frac{g_V}{0.001}\right)^2$ eV
- Scalar (pseudoscalar) disfavoured by ^{8}Be (^{12}C) observation

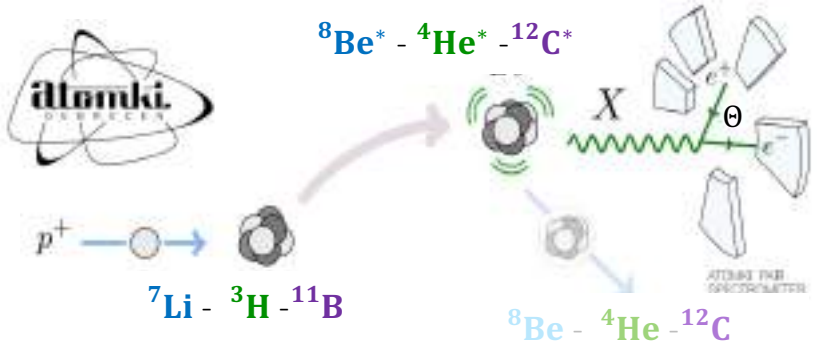

Phys.Rev.Lett. 116 (2016) 4, 042501

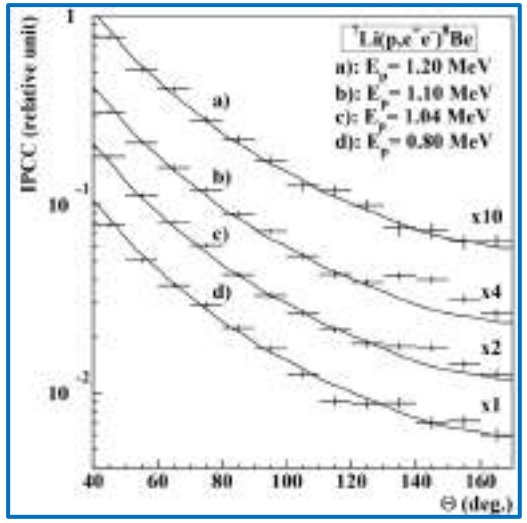

$m_X = (17.01 \pm 0.16)$ MeV

Phys.Rev.C, 104(4):044003

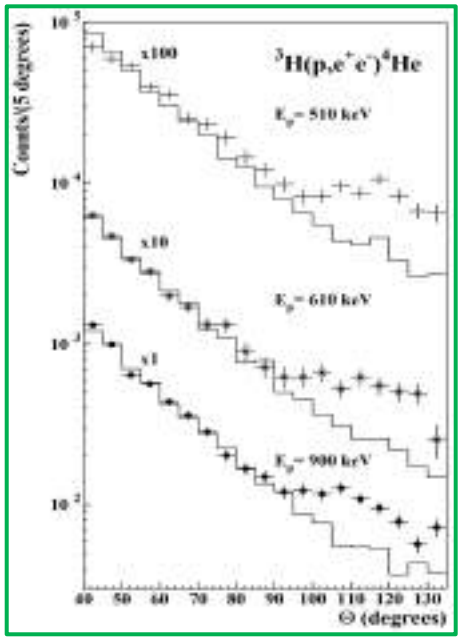

$m_X = (16.98 \pm 0.36)$ MeV

Phys. Rev. C 106, L061601

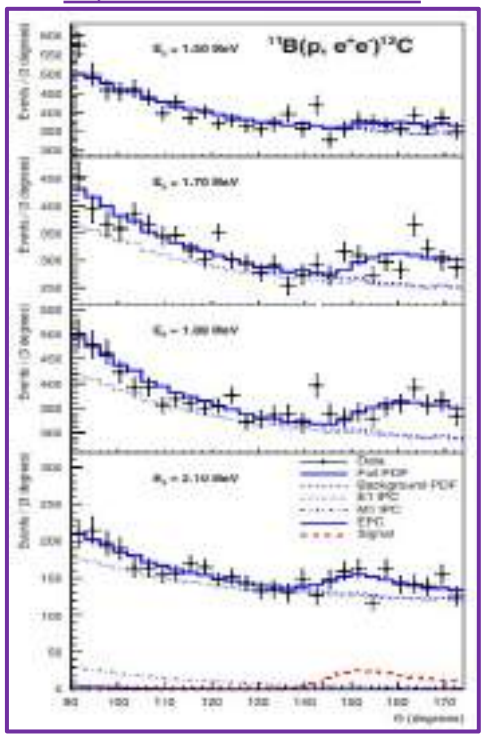

$m_X = (16.86 \pm 0.37)$ MeV

TABLE III. Nuclear excited states N_*, their spin-parity J^P_*, and the possibilities for X (scalar, pseudoscalar, vector, axial vector) allowed by angular momentum and parity conservation, along with the operators that mediate the decay and references to the equation numbers where these operators are defined. The operator subscripts label the operator's dimension and the partial wave of the decay, and the superscript labels the X spin. For example, $\mathcal{O}^{(0)}_{4e}$ is a dimension-four operator that mediates a P-wave decay to a spin-0 X boson.

N_*	J^P_*	Scalar X	Pseudoscalar X	Vector X	Axial Vector X
^{8}Be(18.15)	1^+	...	$\mathcal{O}^{(0)}_{4e}$ (27)	$\mathcal{O}^{(1)}_{4e}$ (37)	$\mathcal{O}^{(1)}_{3e}$ (29), $\mathcal{O}^{(1)}_{5e}$ (34)
^{12}C(17.23)	1^-	$\mathcal{O}^{(0)}_{4e}$ (27)	...	$\mathcal{O}^{(1)}_{3e}$ (29), $\mathcal{O}^{(1)}_{5e}$ (34)	$\mathcal{O}^{(1)}_{4e}$ (37)
^{4}He(21.01)	0^-	...	$\mathcal{O}^{(0)}_{3e}$ (39)	...	$\mathcal{O}^{(1)}_{4e}$ (40)
^{4}He(20.21)	0^+	$\mathcal{O}^{(0)}_{3e}$ (39)	...	$\mathcal{O}^{(1)}_{4e}$ (40)	...

Neutrino Constraints and the ATOMKI X17 Anomaly

An analysis with the angular data alone of 11 different measurements finds that the data is well described by a new particle of mass $m_X = 16.85 \pm 0.04$ MeV with an internal goodness-of-fit of 1.8σ calculated from Wilks' theorem at $\chi^2/dof = 17.3/10$. We use only the best fit

Phys. Rev. D 108, 015009

Combining the nuclear observations: 11 angular anomalies

Resonant X_{17} search @PADME Run III

- $\sigma_{res} \propto \frac{g_{Ve}^2}{2m_e} \pi Z\, \delta(E_{res} - E_{beam}) \propto Z$ → dominant with respect to alternative signal production processes
- $\sqrt{s}$ has to be as close as possible to the expected mass → fine scan procedure with the positron-beam → expected enhancement in $\sqrt{s}$ over the SM bkg

Phys. Rev. D 97, 095004

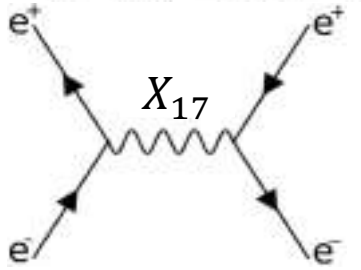

@PADME: X_{17} production through resonant annihilation in diamond target electron: scan around $E_{beam} \sim 282$ MeV aiming to measure 2 body final state yield $N_2(s)$ → e^- at rest approximation leads to large number of X_{17} event

$$N_{vector}^{perPoT} \simeq \frac{g_{Ve}^2}{2m_e} \ell_{tar} \frac{N_A \rho Z}{A} f(E_{res}, E_{beam}) \sim 1.8\times10^{-7} \times \left(\frac{g_{Ve}}{2\cdot10^{-4}}\right)^2 \left(\frac{1\ \text{MeV}}{\sigma_E}\right)$$

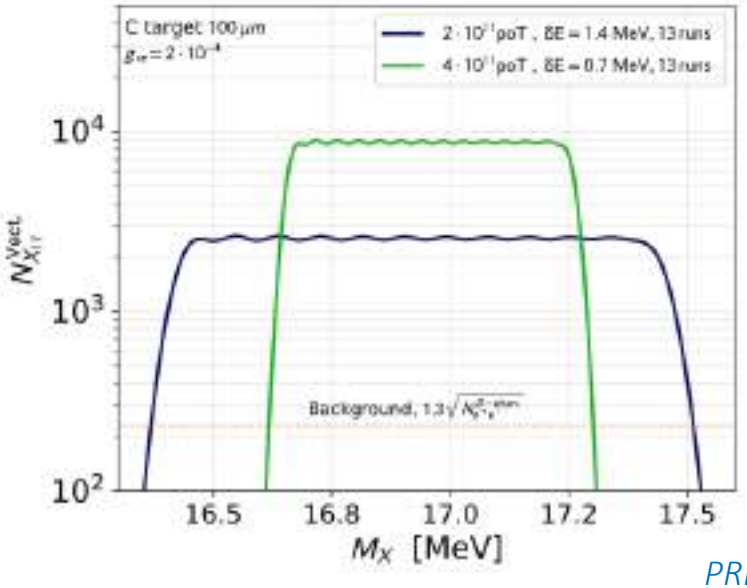

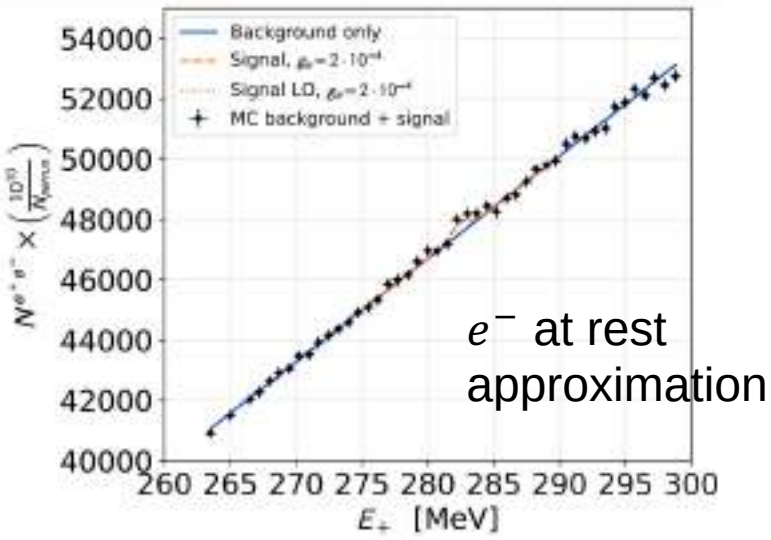

PRD 106 (2022) 11, 115036

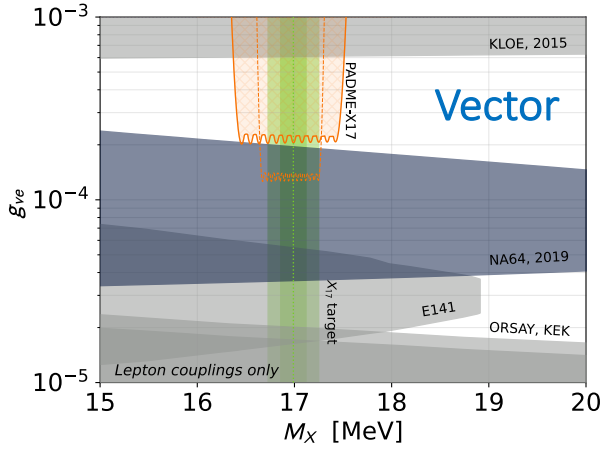

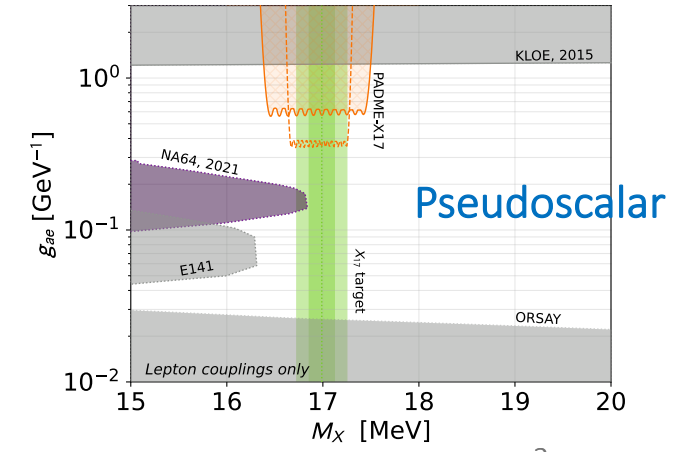

Run III setup

Run III setup for the X_{17} search:

- Active target polycrystalline diamond
- PADME magnetic field off
- ECal: 616 BGO crystals, each $21\times21\times230\ \mathrm{mm}^3$
- Charged particle vetoes not used
- ETagger (scintillator detector) in front of ECal for e/γ discrimination
- Timepix3 high granularity silicon-based detector for beam spot
- LG luminometer (NA62 Large Angle Veto spare block)

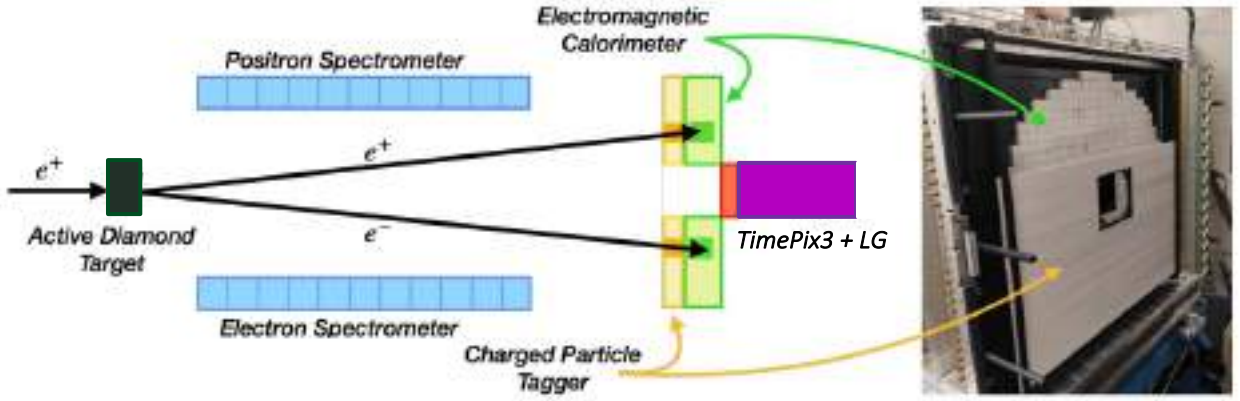

2022 JINST 17 P08032 - arXiv:2405.07203

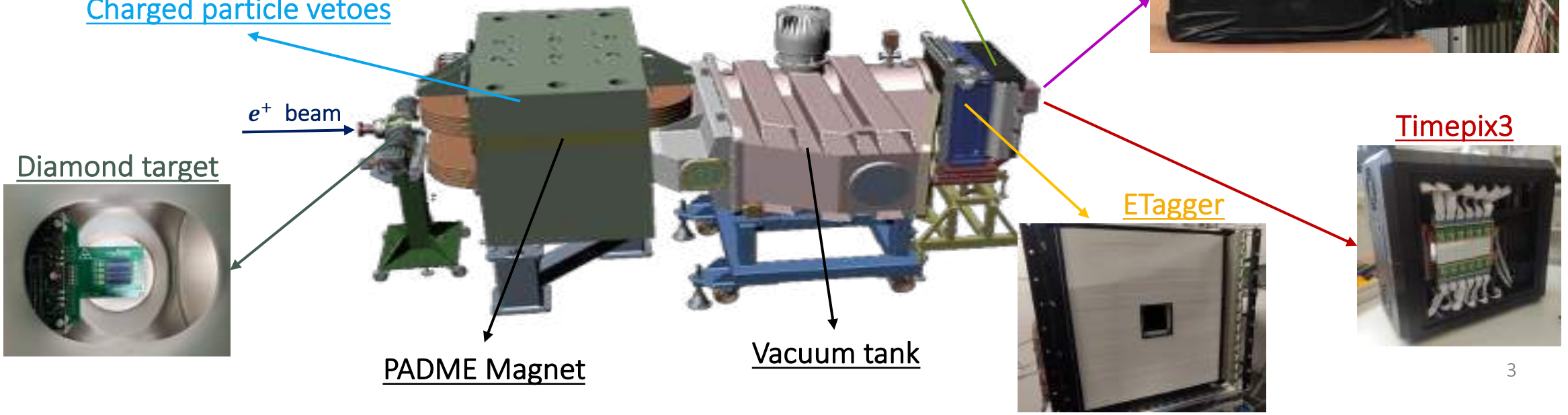

Run III dataset

Total amount of collected data is $\sim 6\times10^{11}$ PoT, i.e. $\sim 10^{10}$ PoT per $\sqrt{s}$ point:

- 42 points in $263\ \text{MeV} < E_{Beam} < 292\ \text{MeV}$ and $\delta E_{Beam} \sim 0.75\ \text{MeV}$ energy step → on-resonance region
- **6 points out-of-resonance,** where the X_{17} production is forbidden:
  - 5 points with $\sim 10^{10}$ PoT each and $205\ \text{MeV} \leq E_{Beam} \leq 212\ \text{MeV}$
  - 1 point with $\sim 2\times10^{10}$ PoT and $E_{Beam} = 402\ \text{MeV}$

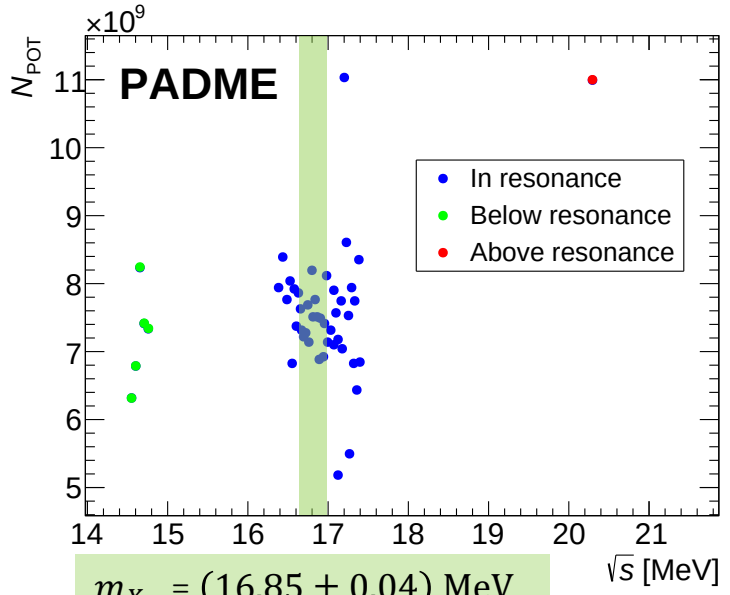

$m_{X_{17}} = (16.85 \pm 0.04)\ \text{MeV}$

Phys. Rev. D 108, 015009

Some terminology:

- **Period**: a scan point at a fixed beam energy, typically lasting 24 hours
- **Scan**: a chronological set of periods typically decreasing in energy
- Scan 1 and 2 periods spaced $1.5\ \text{MeV}$ but relatively **interspersed**
  - Scan 1: 12/10/2022- 10/11/2022
  - Scan 2: 25/11/2022- 21/12/2022
- Detailed Geant4-based MC performed for each period

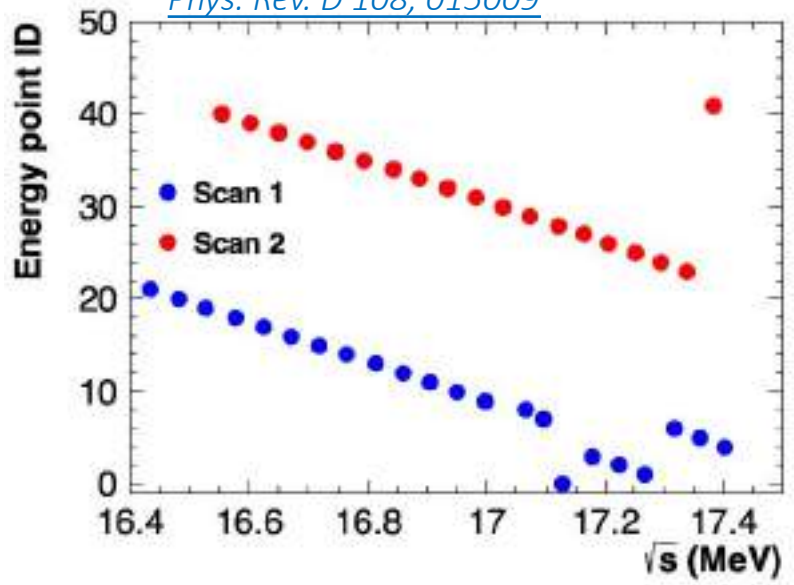

Run III analysis inputs

Signal + bkg hypothesis → $\overbrace{N_2(s) / N_{PoT}(s)\, B(s)}^{g_R(s)} = K(s)[1 + S(s; M_X, g_{Ve})\, \varepsilon_S(s)/ B(s)]$

To be compated with

Bkg only hypothesis → $N_2(s) / N_{PoT}(s)\, B(s) = K(s)$

Analysis inputs:

- $K(s)$ → DATA-MC scale factor expected linear in $\sqrt{s}$
- $N_2(s)$ → number of 2-body final states in ECal
- $N_{PoT}(s)$ → number of e^+ on target from LG beam-catcher
- $B(s)$ → expected background yield per PoT
- $S(s; M_X, g_{Ve})$ → expected signal production per PoT for {mass, coupling} = {M_X, g_{Ve}}
- $\varepsilon_S(s)$ → signal acceptance and selection efficiency

Measure and evaluate systematic errors on:

- N_2 (bkg subtracted) on data
- PoTs
- Bkg Yield
- Signal efficiency & shape

g_R systematics error budget in Run III

Uncorrelated uncertainty on $g_R(s)$ = $N_2(s)$ / ($N_{PoT}(s)$ $B(s)$)

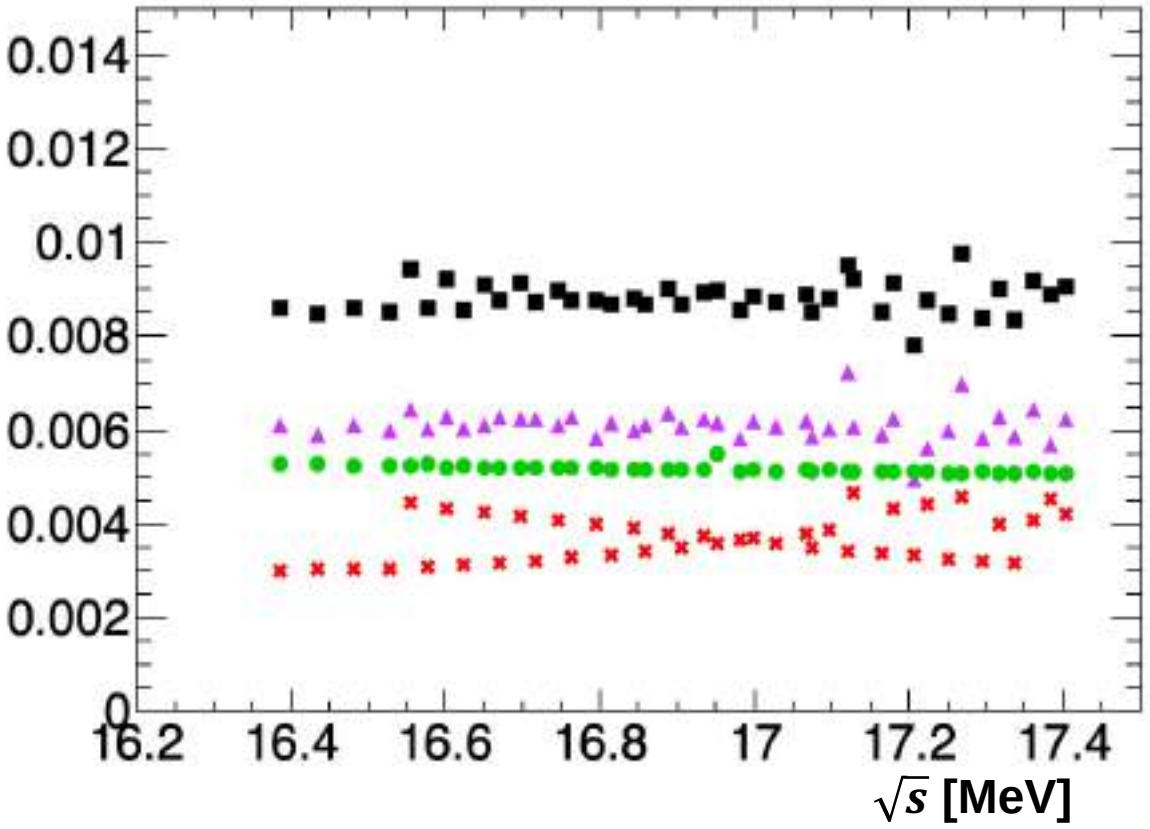

JHEP 11(2025), 007

Uncorrelated errors

Source	Uncertainty (% per energy point)
$N_2(s)$	0.60
$B(s)$	0.54
$N_{\mathrm{PoT}}(s)$	0.35
Total on $g_R(s)$	0.88

$K(s)$, constant term

Source	Uncertainty (%)
Lead-glass calibration	2.0
Absolute B yield	1.8
Energy-loss correction to N_{PoT}	0.5
Radiation-induced correction to N_{PoT}	0.3
Total	2.8

$K(s)$, $\sqrt{s}$-slope

Source	Expected value (%/MeV)
Radiative corrections	$-0.6 \pm 0.2 \pm 0.6$
Total	-0.6 ± 0.6

Next step: Is $g_R(s)$ compatible with $K(s)$ or $K(s)$ [1+ $S(s)$ $\varepsilon_S(s)/B(s)$]?

Expected sensitivity

Expected 90% CL UL in absence of signal:

- Modified frequentist approach, LEP-style test statistic. **Likelihood fits** performed for **signal + background** vs **background** only
- Total error budget: $\delta g_R(s)=0.88\%$ and $\delta K(s)=2.8\%$
- For a M_X: $CL_s = \frac{P_S}{1-P_B}$ to define the UL on g_{Ve}

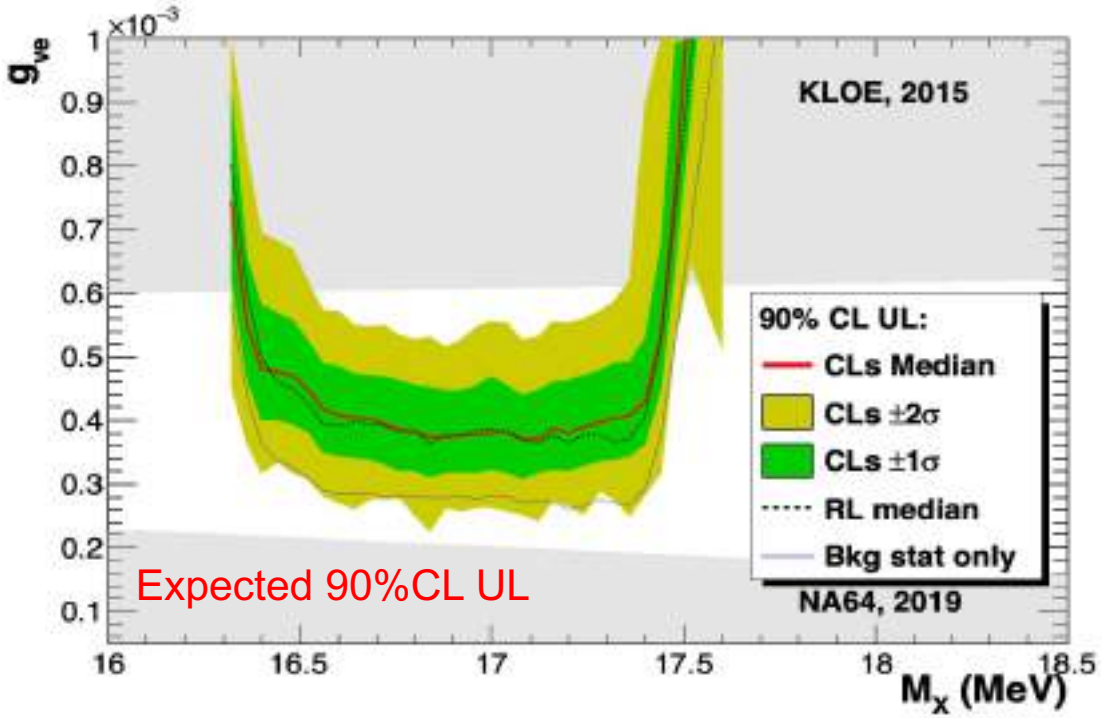

Before box opening, error estimate validation (*JHEP 06 (2025) 040*):

- Aim to blindly define a sideband in $g_R(s)$, excluding 10 periods of the scan
- Define the masked periods by optimizing the probability of a linear fit in $\sqrt{s}$

The “blind unblinding” technique

Define the masked periods by optimizing the probability of a linear fit in $\sqrt{s}$

1.Threshold on the χ^2 fit in side-band is $P(\chi^2) = 20\%$

2.If ✅, check if the fit pulls are gaussian

3.If ✅, check if a straight-line fit of the pulls has no slope in $\sqrt{s}$ (within 2σ)

4.If ✅, check if constant term and slope of the linear fit for $N_2(s)/B(s)$ are within 2σ of the expectations

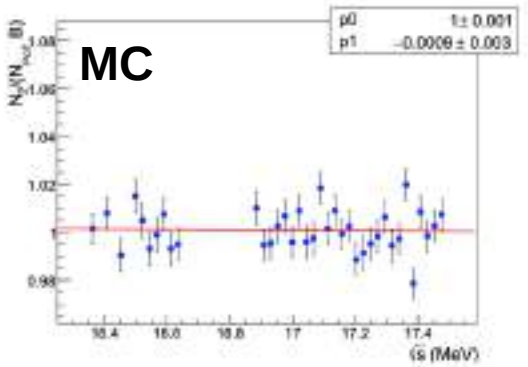

Successfully applied: *JHEP 11(2025), 007*

1. $P(\chi^2) = 74\%$
2. Pulls gaussian fit probability: 60%
3. Slope of pulls consistent with zero
4. Constant term: $1.012(2)$ vs $1.00(3)$
   Slope: $(-0.010 \pm 0.005)\ \mathrm{MeV}^{-1}$ vs $(-0.006 \pm 0.006)\mathrm{MeV}^{-1}$

Ready to unblind

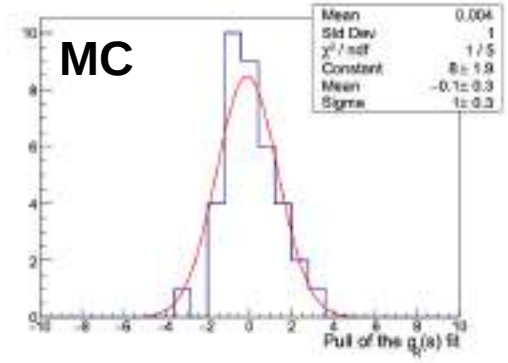

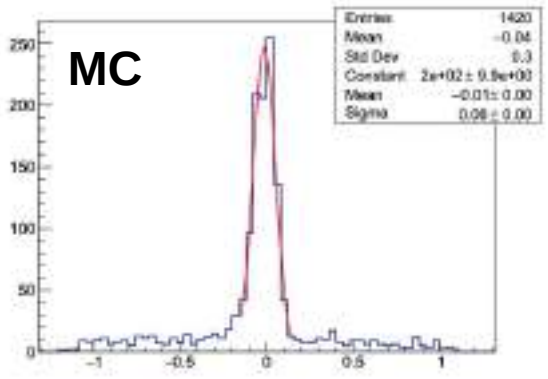

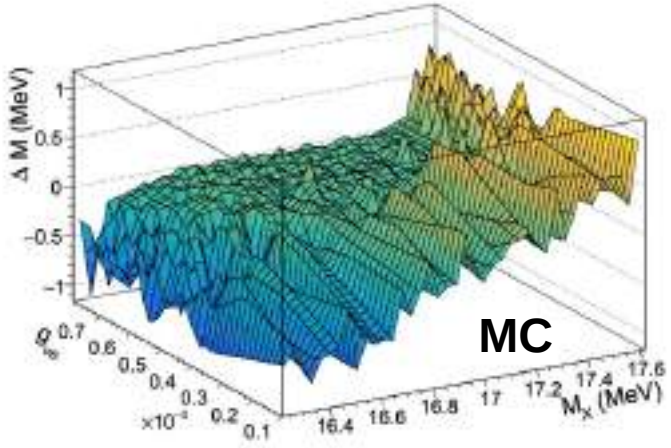

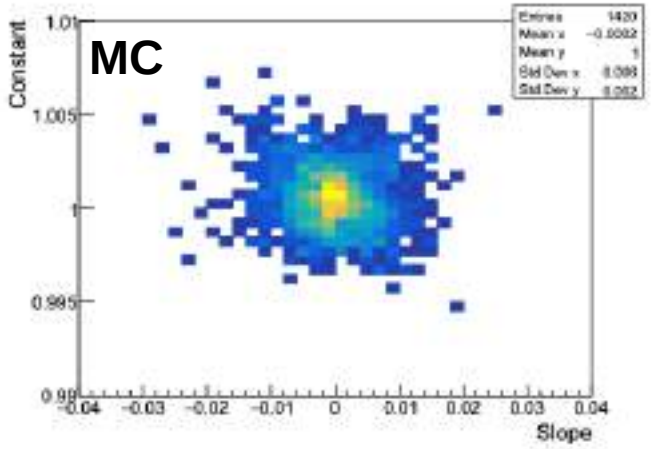

Run III result and outcome

Some excess is observed beyond the 2σ global coverage (2.5σ local)

- At $M_X = 16.90(2)$ MeV, $g_{Ve} = 5.6\times10^{-4}$, the global probability dip reaches $3.9^{+1.5}_{-1.1}\%$, corresponding to $(1.77 \pm 0.15)\sigma$ one-sided (look-elsewhere calculated exactly from the toy pseudo-events)
- Assuming a 3σ interval around the expected $M_X = 16.85(4)$ MeV (*PRD 108, 015009 (2023)*), p-value dip deepens to $2.2^{+1.2}_{-0.8}\%$ corresponding to $(2.0 \pm 0.2)\sigma$ one-sided

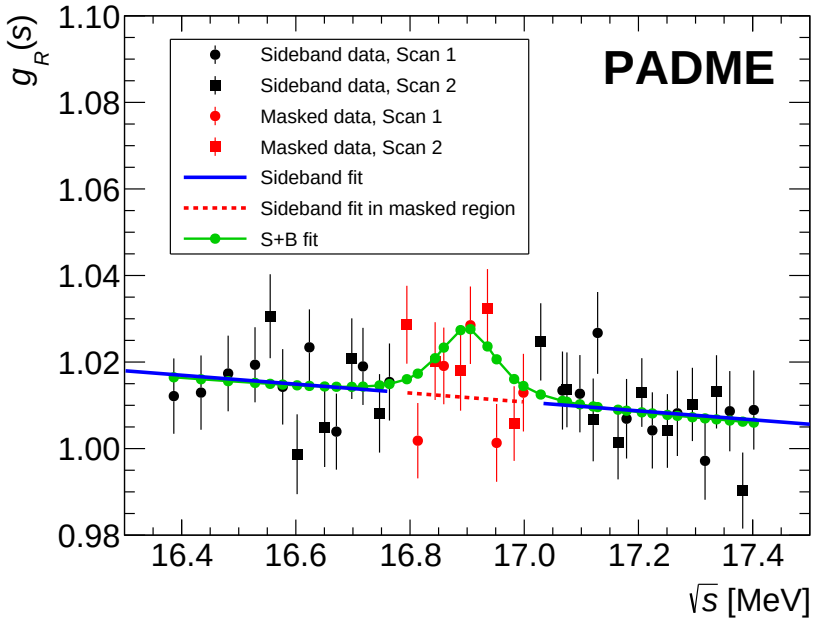

JHEP 11(2025), 007

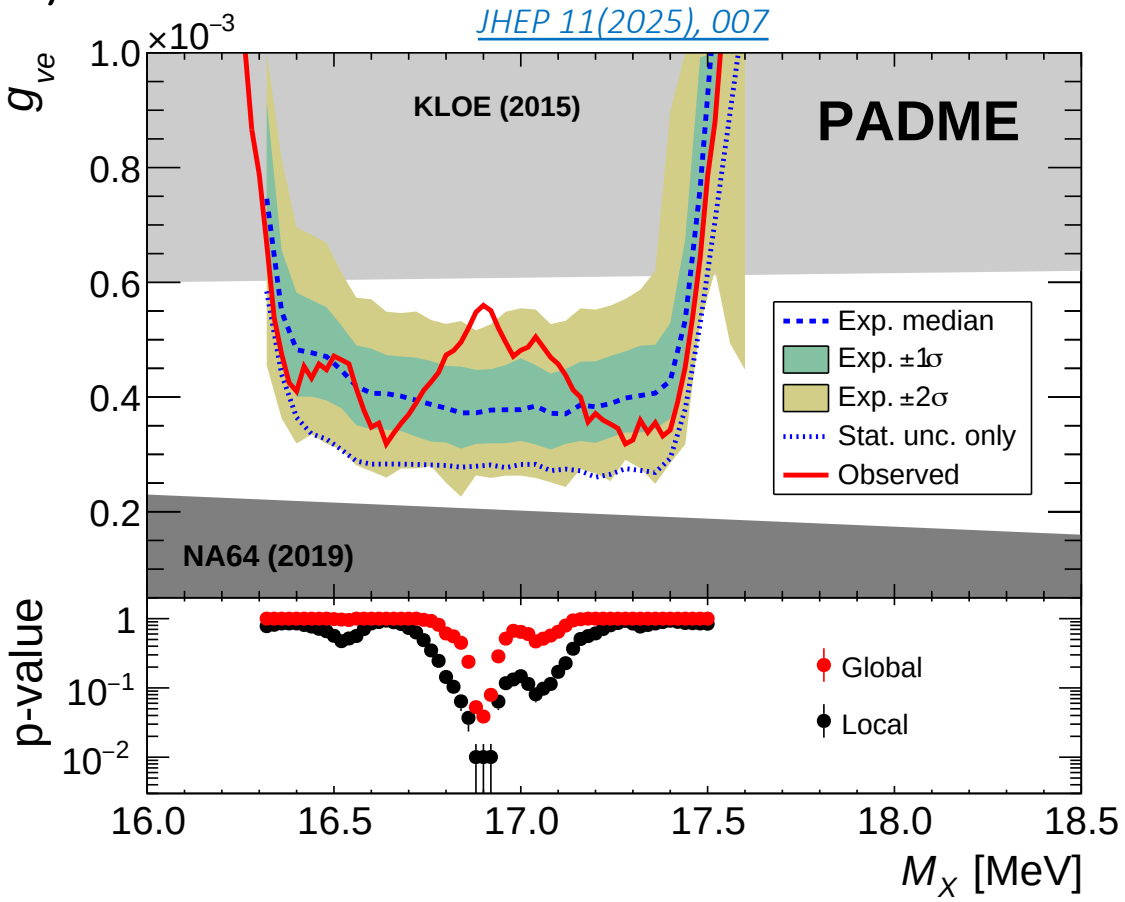

Need for more data → Run IV data taking in 2025

Lessons from Run III

The main Run III exclusion limitations arose from:

$N_2(s)$

- Per point statistics acquired → 2x N_{PoT} and need for acceptance improvement
- Remnant PADME magnetic field $\mathcal{O}(10\ \mathrm{G})$ → Total de-gaussing procedure

$B(s)$

- SM bkg due to $e^+e^- + \gamma\gamma$ → PID to remove neutral bkg + $e^+e^- \to \gamma\gamma$ to normalise
- Beam spot variation → redundancy on the beam spot monitoring

$N_{PoT}(s)$ limited by two main systematics:

- **Radiation-induced loss** → online degradation monitor to correct
  - Prompt observable → Energy deposit in ECal, Q_{LG} and Q_{Target}
- **Passive material (inside Timepix) crossing** → lighter beam monitor detector with larger active area
  - Dedicated test beam + MC simulation to confirm

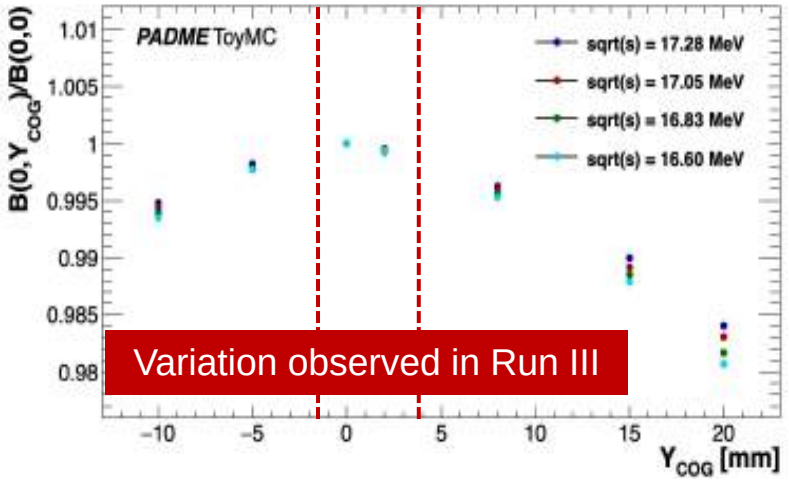

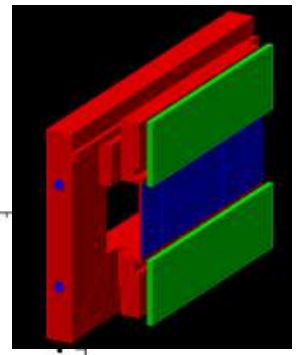

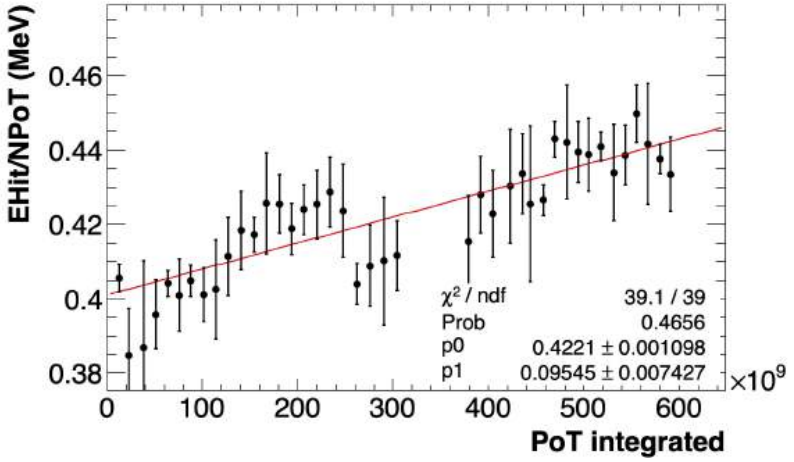

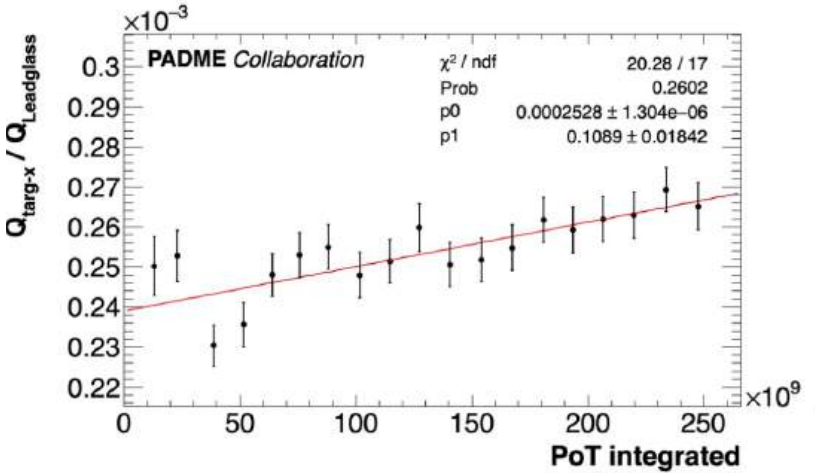

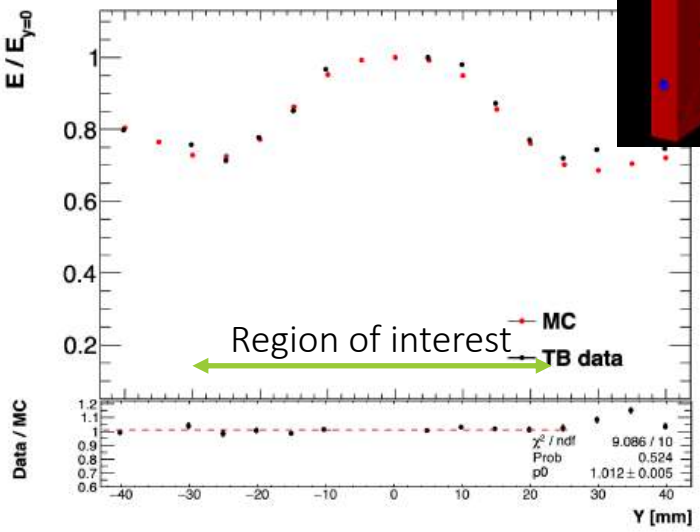

Run IV improvements overview

Run IV paradigm → increase sensitivity to confirm/disprove Run III result

- Diamond target position moved downstream by ~ 30 cm + position readout changed
- Passive material removed and PADME Magnet fully degaussed → remnant $B_{PADME} < 1\text{G}$
- New detectors:
  - PadMMe Micromegas chamber replaces the ETagger
  - TMM Micromegas replaces the TimePix beam monitor
  - Radiation-induced loss monitor system for online LG calibration (2nd LG block + LED pulser)

Diamond target

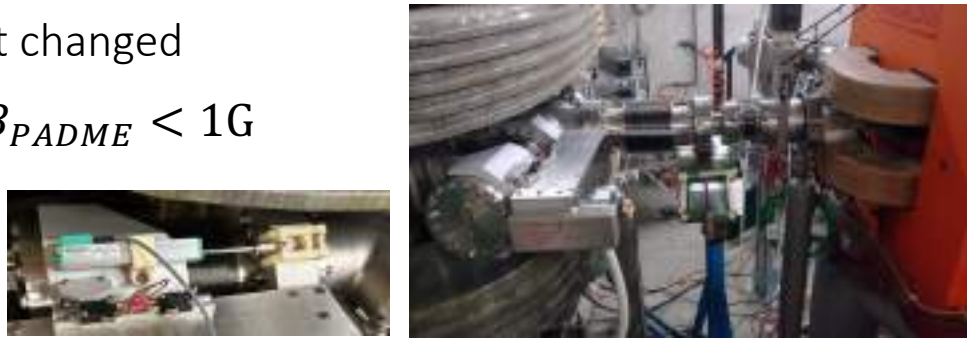

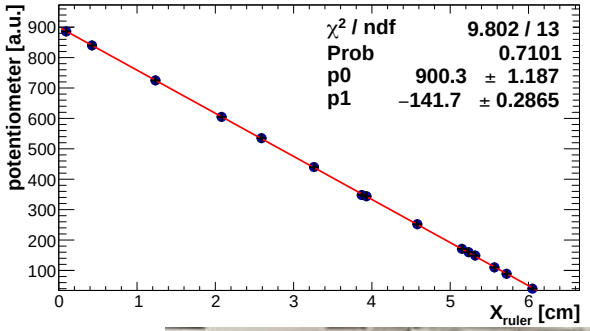

Source	Uncertainty [%]	
	Run III	Run IV target
N_2	0.6	0.3
B	0.35	0.3
N_{PoT}	0.55	0.3
TOTAL	0.88	0.5

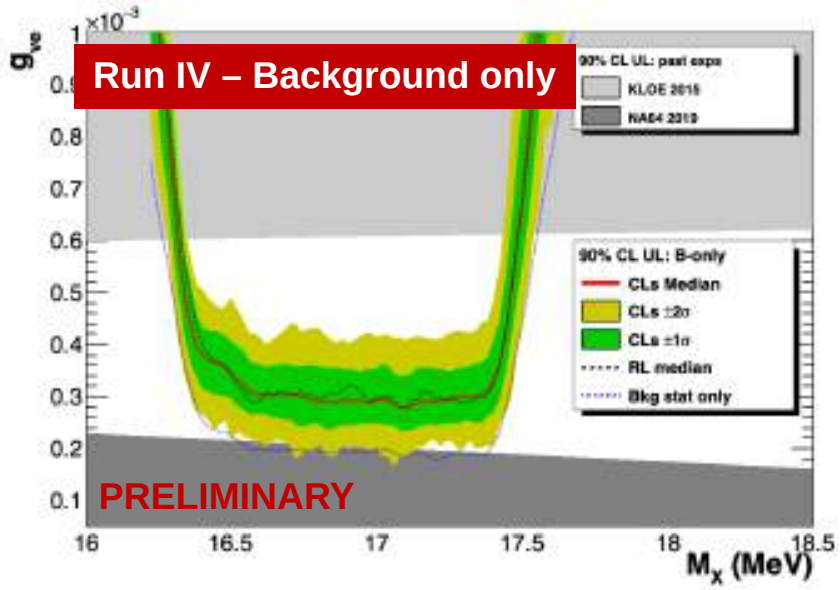

Exclusion estimate: Run III dataset + systematics lowered

PadMMe

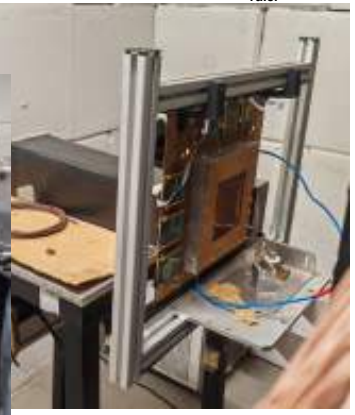

TMM

Diamond target – Run IV acceptance

Run period	Target-ECal [mm]	Scattering θ_{lab} [mrad]	Magnet bore shadow
Run III	3700	24 - 73	249 mm
Run IV	3360	27 - 82	268 mm

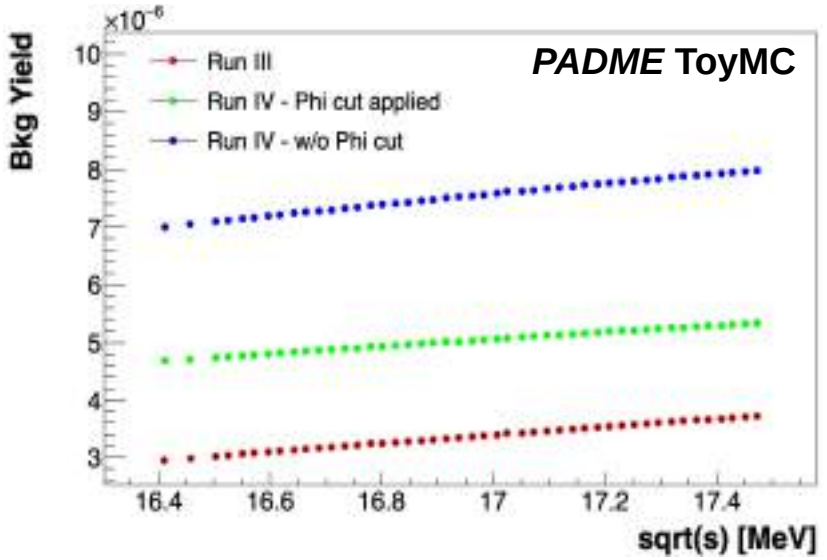

- Target thickness measurement dedicated data taking campaign
- Phi-cut can be totally removed or adapted
- Acceptance region widened → $\frac{Sig}{\sqrt{Bkg}}$ increases
- Run-by-run Run IV integrated luminosity increases by a factor of ~ 2.5 wrt Run III
  - Run III: $N_2 = 3.705 \times 10^{-6}$ (evaluated over 0.78×10^{10} PoT)
  - Run IV: $N_2 = 9.948 \times 10^{-6}$ (evaluated over 10^{10} PoT)

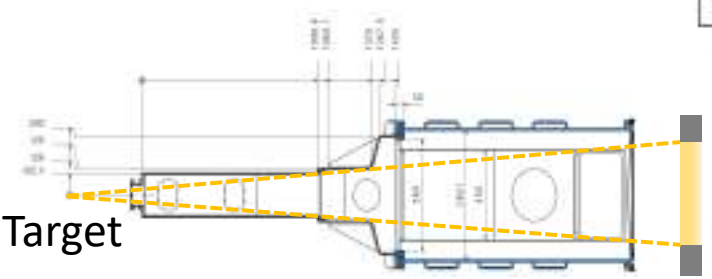

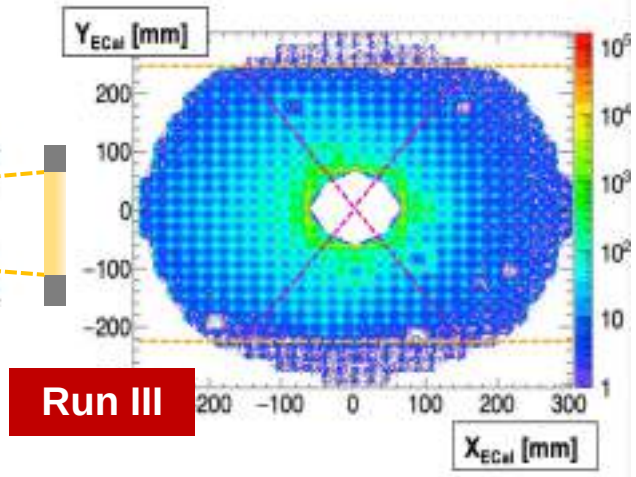

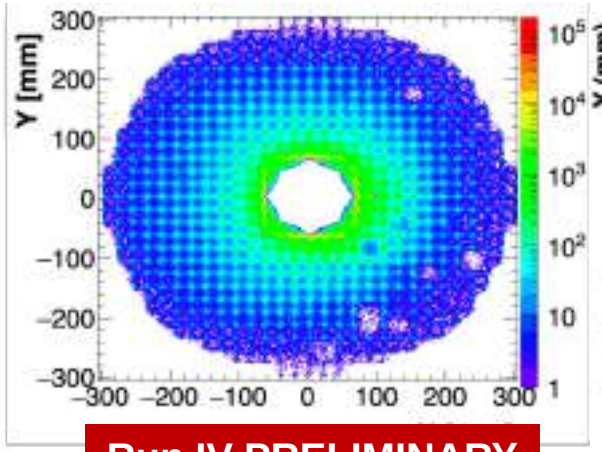

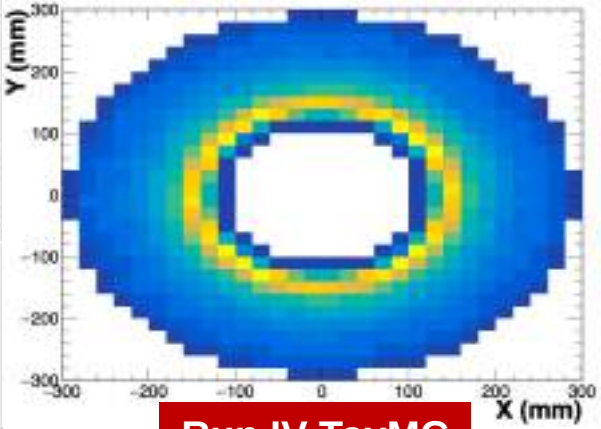

Run IV data taking

Energy scan technique as in Run III – 39 scan points collected + 15 no-target

	Run III	Run IV
Scan points	42 around resonance Scan 1 – 22 points / Scan 2 – 20 points	36 around resonance Scan 1 and 2 – 18 points each
N_{PoT}	$\sim 0.8\times10^{10}$ PoT per on-resonance-point	$\sim \mathbf{2.2\times10^{10}}$ PoT per on-resonance-point
E_{Beam}	$263\ MeV < E_{Beam} < 292\ MeV$ and $\delta E_{Beam} \sim 0.75\ MeV$	$\mathbf{268\ MeV < E_{Beam} < 295\ MeV}$ and $\boldsymbol{\delta E_{Beam} \sim 0.75\ MeV}$
Below resonance	5 points $@205 - 212\ MeV$	1 point $@\mathbf{260\ MeV}$
Above resonance	1 point $@402\ MeV$	2 points $@\mathbf{300 - 330\ MeV}$

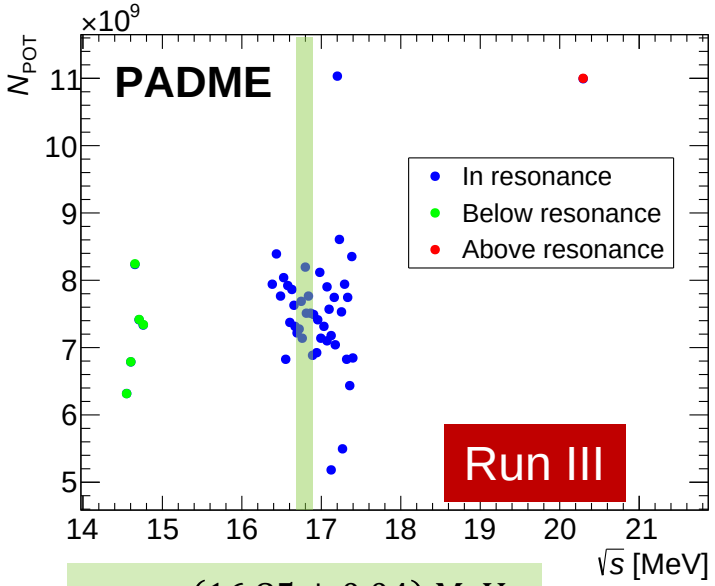

$m_{X_{17}}$ = (16.85 ± 0.04) MeV

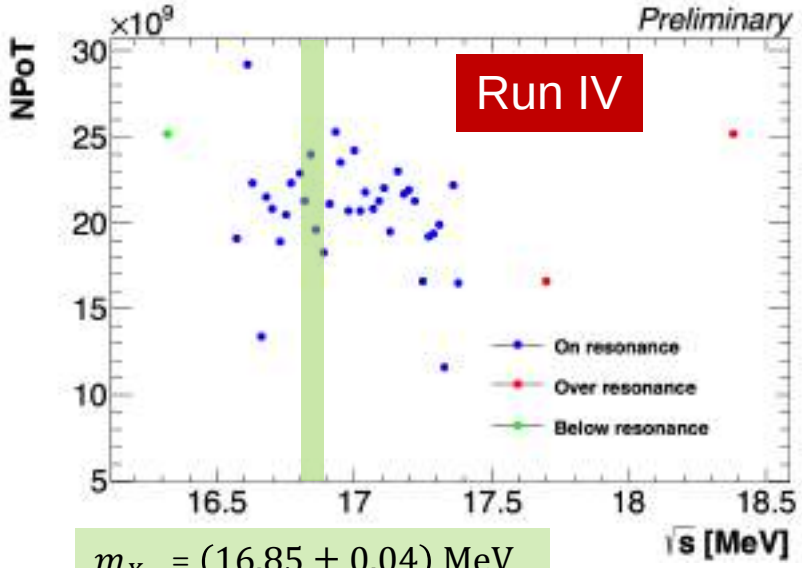

$m_{X_{17}}$ = (16.85 ± 0.04) MeV

Phys. Rev. D 108, 015009

Target reconstruction optimisation

Target waveforms are affected by common-mode noise:

- Channel-by-channel **different noise pattern**
- Beam-NoBeam different structure
- Induced capacitance effects on strips nearby the beam-fired strips

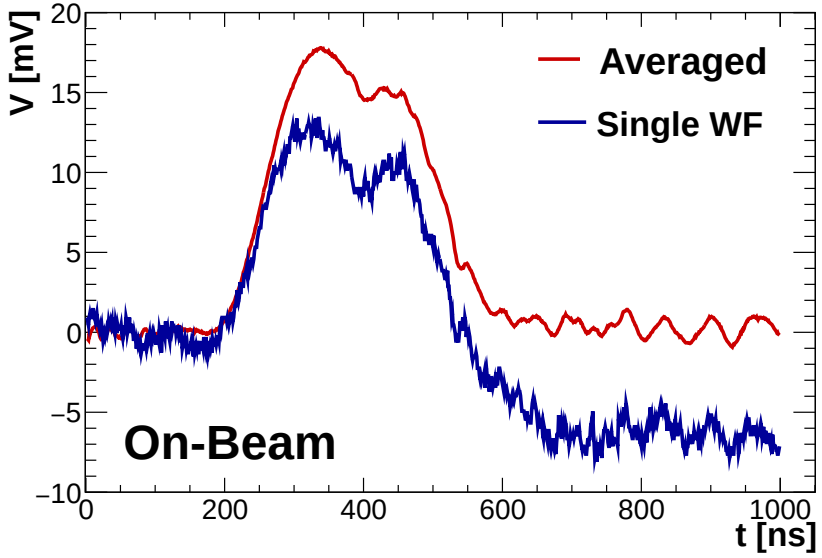

Averaged waveform over $\mathcal{O}(100)$ wf mitigating the random noise structures

$$V_{cum}(t) = \frac{1}{N_{cum}} \times \left[\sum_{i=0}^{N_{cum}} V_i(t) - \sum_{i=0}^{N_{cum}} \left(\frac{1}{N_{ped}} \sum_{t=0}^{t_{ped}} V(t) \right)_i \right]$$

Charge integration: $Q = \sum_{t_{start}}^{t_{stop}} \frac{V(t)}{Z}$ (if $V(t) \leq 0 \Rightarrow V(t) = 0$)

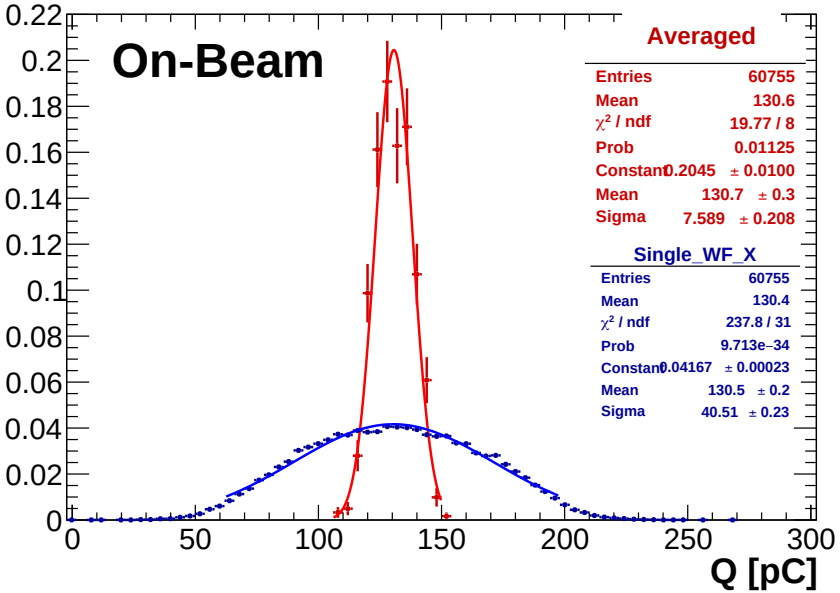

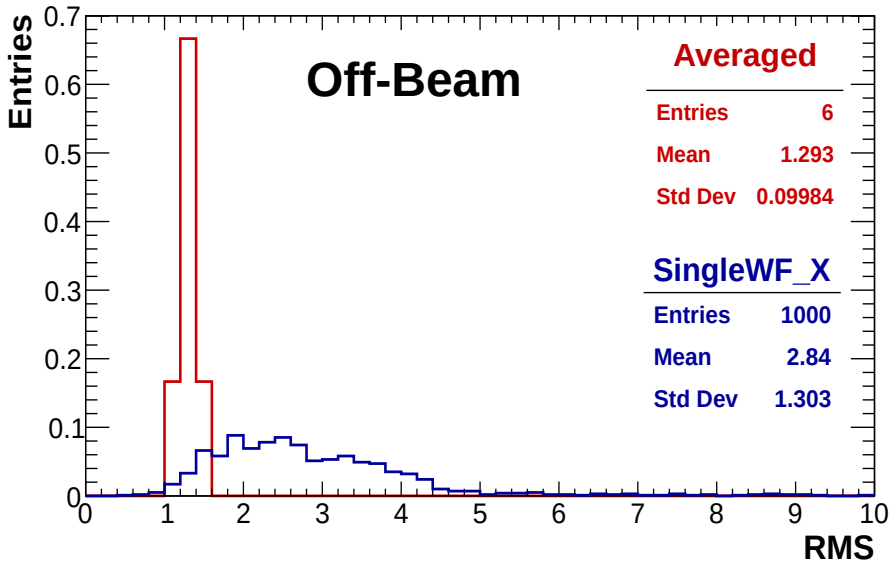

Target X-strip position scan

- Beam focused @Target and kept stable → Central strip and first neighbours fired
- Target moved by 1 mm
- Calibration constants obtained minimising

$$\chi^2 = \sum_{runs} \sum_{i-1}^{i+1} \frac{\left[k_i q_i^{tar,bare} - Q_{LG} f_i(\mu,\sigma)\right]^2}{\sigma_{Q_{LG}}^2}$$

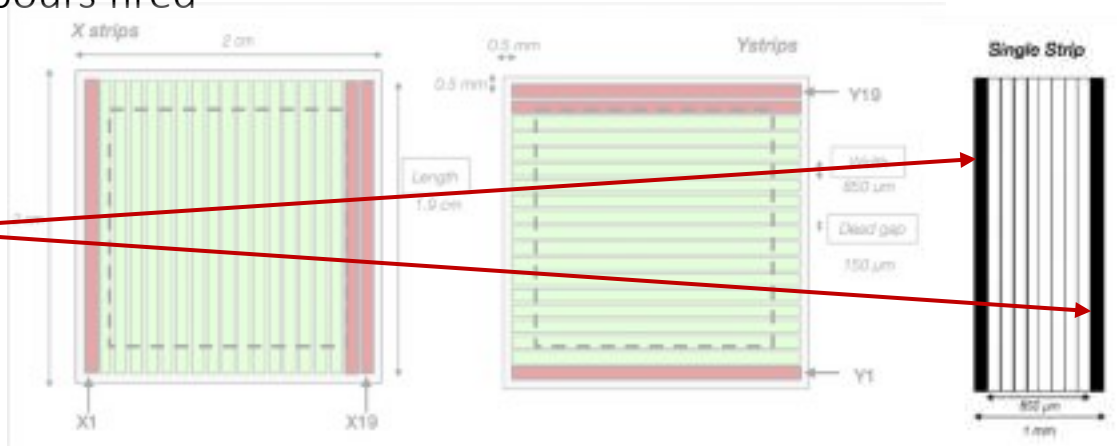

1. Each run provides:
   - The three relevant un-calibrated cumulative target charges $q_i^{tar,bare}$
   - Leadglass mean charge Q_{LG} obtained averaging over N_{cum}
2. $f_i(\mu,\sigma)$ accounts for the charge loss in death areas (15% of each strip)
   - Beam shape approximated as a Gaussian
3. All runs are collected into a global χ^2 with 18 parameters
   - 16 coefficients k_i
   - Beam position μ and width σ assumed fixed for the entire run
4. Minimise χ^2 getting calibration constants

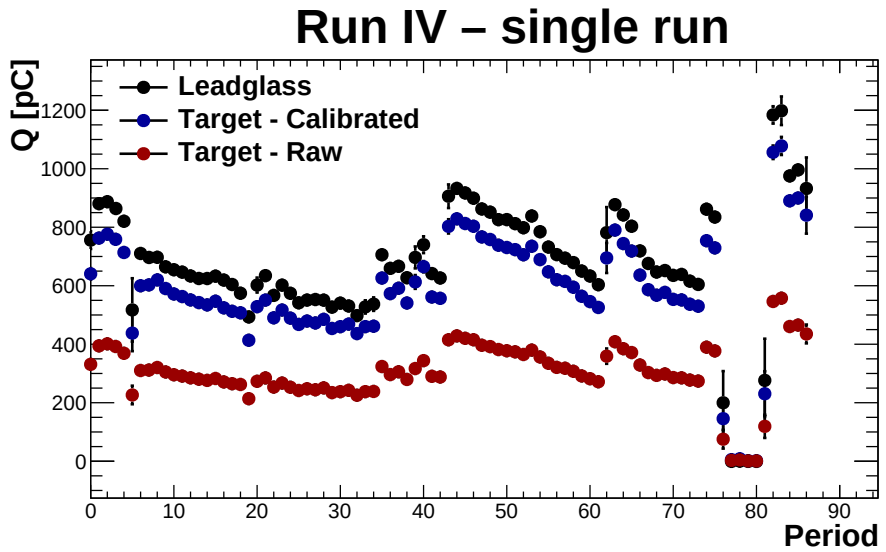

PadMMe – Micromegas tracker

- e/γ discrimination → bkg reduced by 20% - charged final states only
- Access to different observables N_2/N_{PoT}, ee/N_{PoT}, $ee/\gamma\gamma$
- Tag and probe improves
- Main features:
  - 65x65x10 cm^3 - gas mixture (Ar:CF4:Iso=88:10:2)
  - 2 RO planes divided into 2 PCBs vertically(horizontally) separated P1(P2)
  - Hit efficiency > 90%
- **Beam monitor capability** → central region at low gain (orange+green)
  - Used as online monitor during Run IV data taking
- **Need to face very high occupancy**

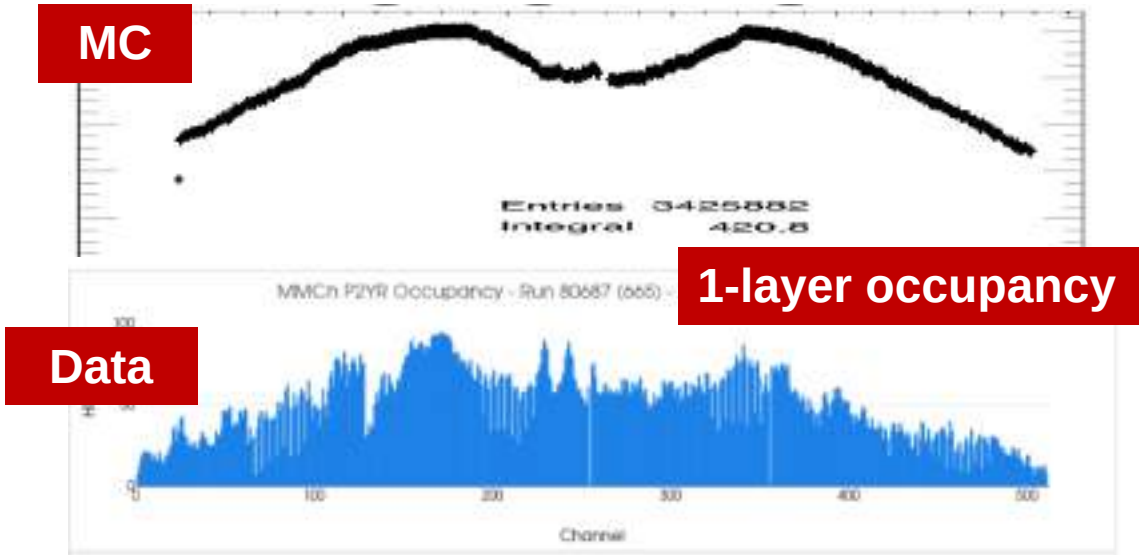

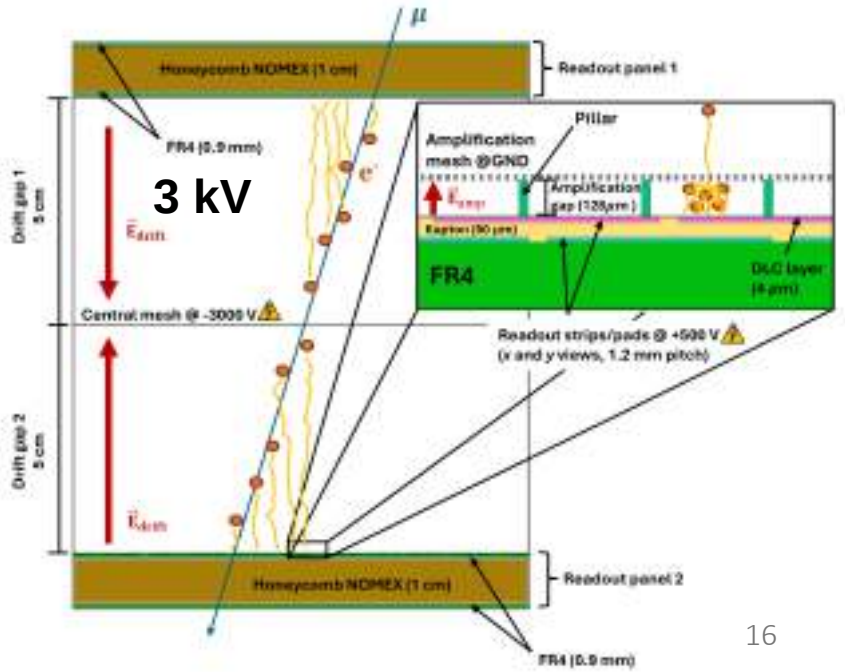

PadMMe – Micromegas tracker

- Huge **combinatory** in pattern recognition
  - ~3500/4096 fired strips ~85% occupancy
  - ~200 track candidates found w/o Interaction Point (IP) constraint
    → **IP oriented pattern recognition algorithm**
- Each charged particle measured in 2 planes – both X and Y coordinates
  - 4 tracks (2D) expected for charged particle, so-called Level-0 tracks
  - High efficiency but a Level-0 track requirement has high bkg component (combinatorial tracks)
  - Need at least 2/3 out of 4 coincidence
  - **Level-1 track**: two-plane coincidence
  - Performances obtained with nominal Run IV beam intensity

Lateral view

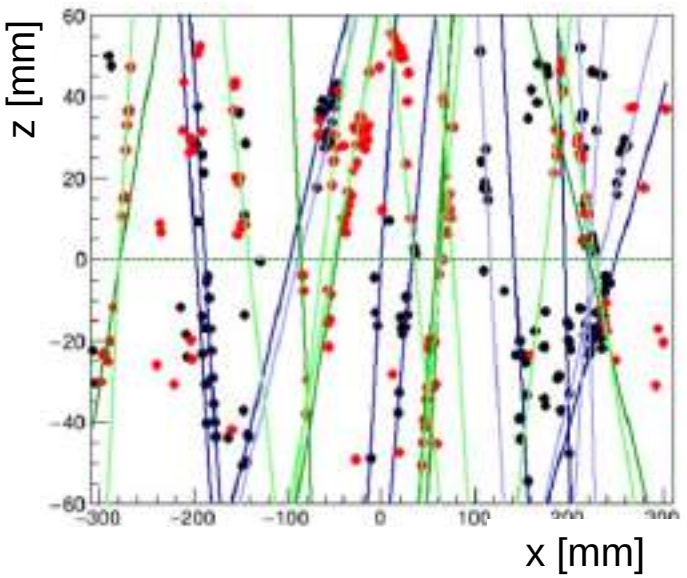

X,Y direction track residual

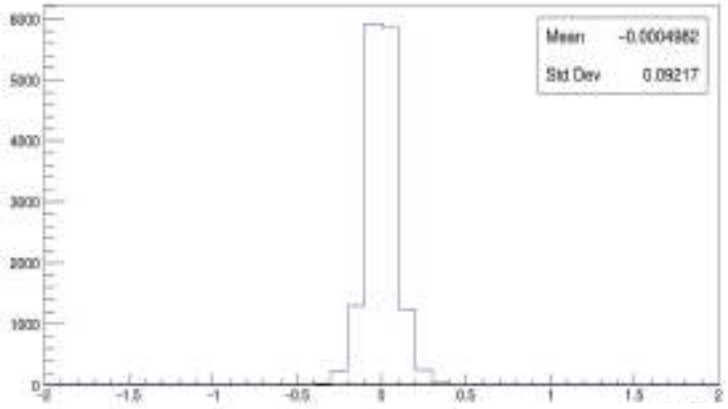

$\sigma_{x,y} \simeq 100\ \mu m$

Z direction track residual

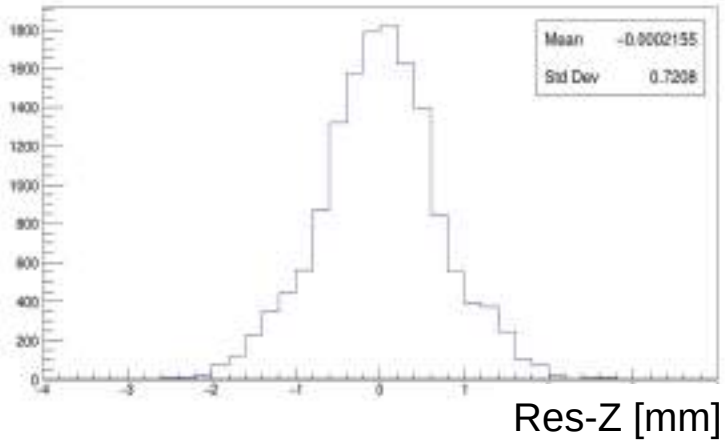

$\sigma_z \simeq 700\ \mu m$

Track to ECal cluster association

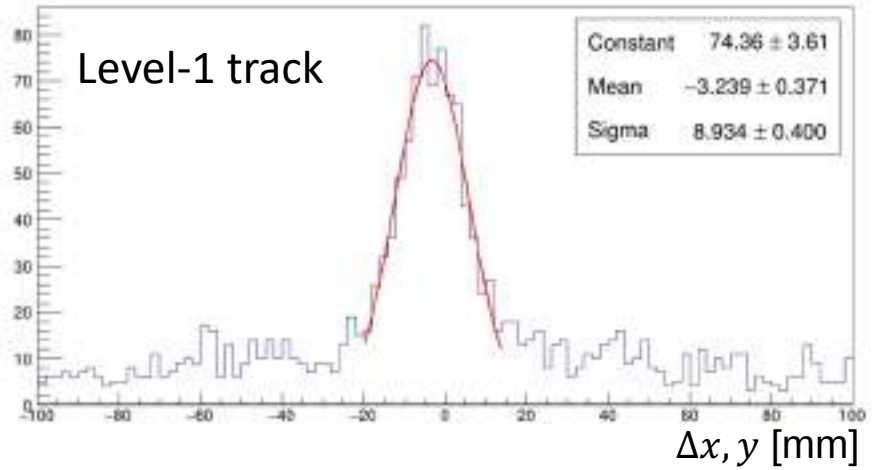

$\sigma_{x,y} \simeq 9\ mm$

TMM – beam monitor detector

- A 10x10x5 cm^3 micromegas detector:
  - Connected in series to the padMMe - same gas mixture (Ar:CF4:Iso=88:10:2)
  - HV 350 V, Drift 300 V
  - Chamber placed in front of the LG
- Larger and unifiorm active area wrt TimePix and less passive material budget
- Beam spot and flux monitor
- Proper metrology alignment **not yet implemented**

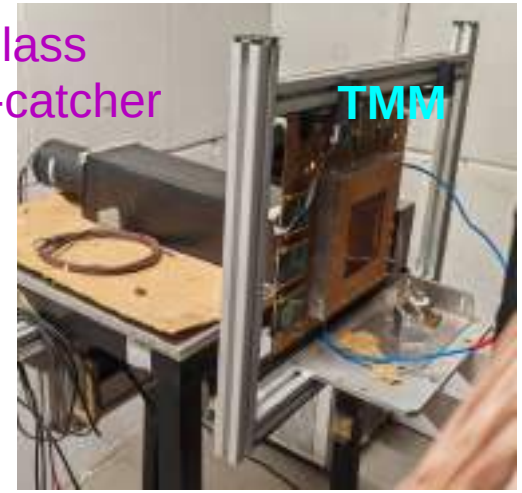

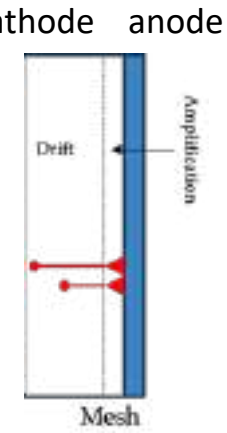

Beam spot at TMM

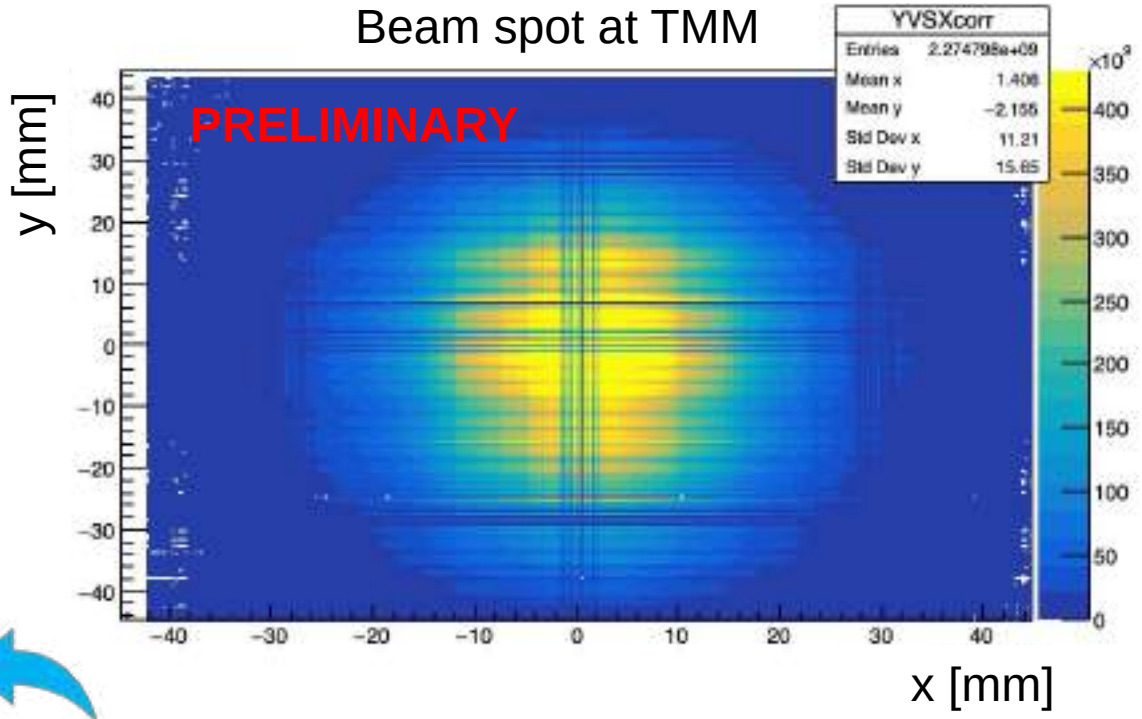

Beam profileX at TMM

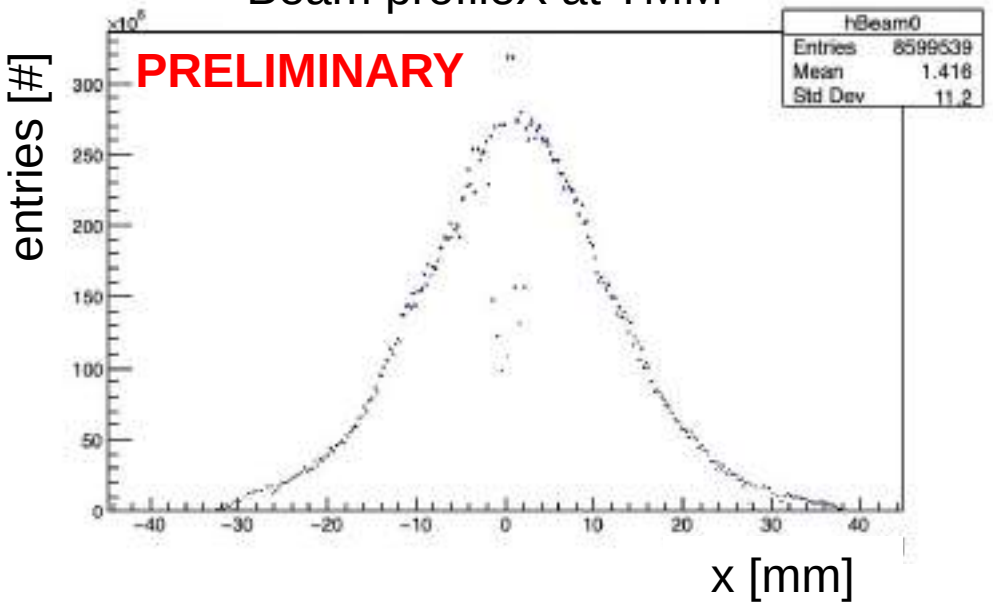

Beam monitor and parameter - Target

- **Beam monitor at 4 different levels** using different methods
  - Aiming at measuring: position, angle, beam spread and beam divergence
- TARGET capabilities:
  - Position evaluated with charged weighted mean over the 3 fired-strips
  - **Beam position stable within 100-150 μm**
  - Complementary measurement of beam flux from collected charge (ongoing)
  - Expected decreasing trend of the beam spread as a function of E_{Beam}

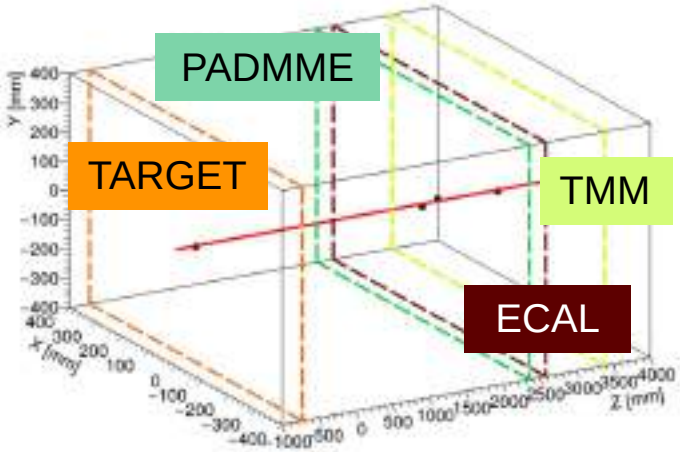

Beam position – X vs RunNumber

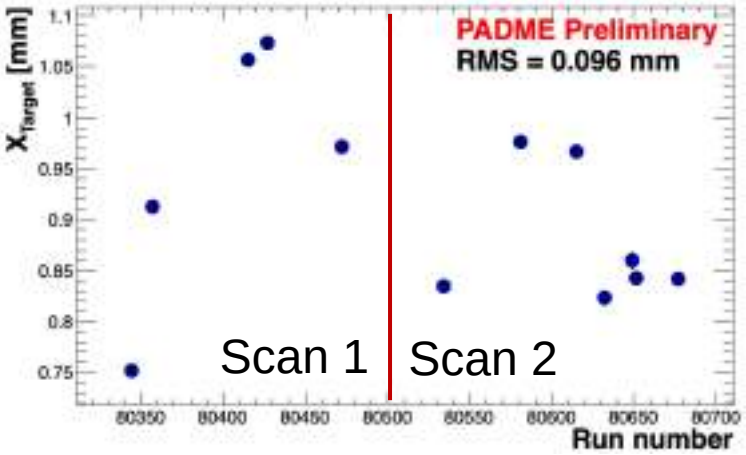

Beam position – Y vs RunNumber

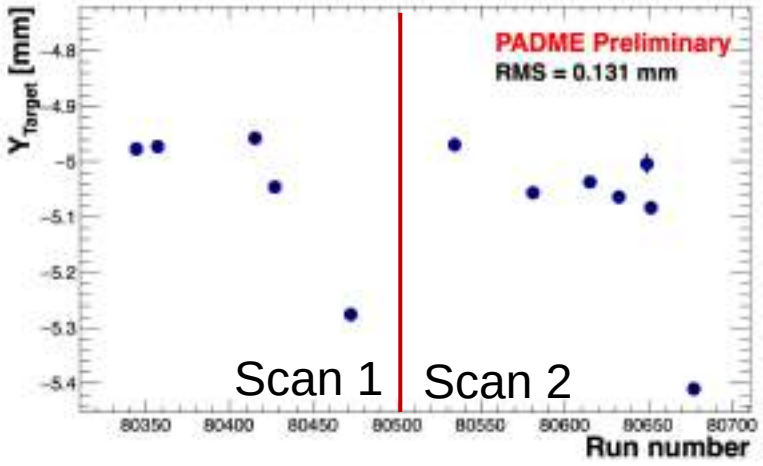

Beam spread @Target vs E_{Beam}

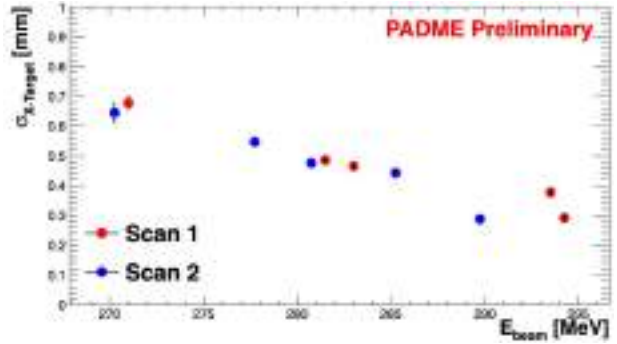

Beam divergence projected @ECal vs E_{Beam}

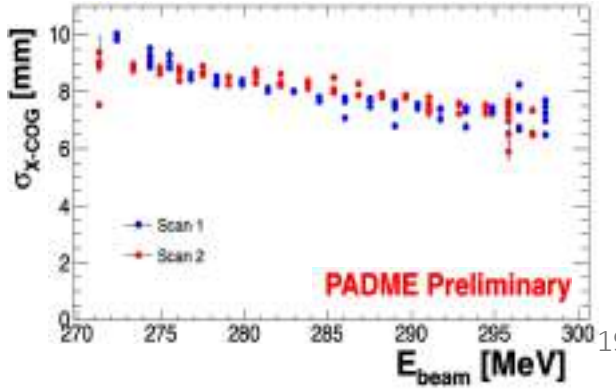

- Sample runs of both Scan 1 and 2 analysed (first ~ 30 min)
- Y strip calibration and equalization still missing

LG radiation-induced loss monitor

Run III N_{PoT} determination affected by **radiation-induced loss**

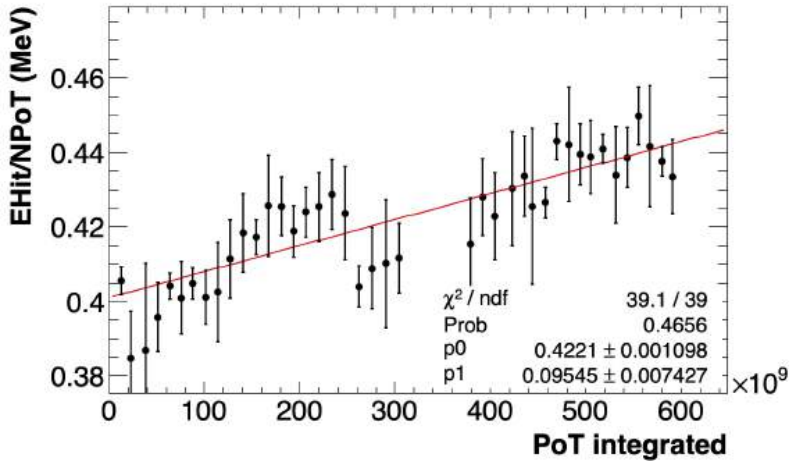

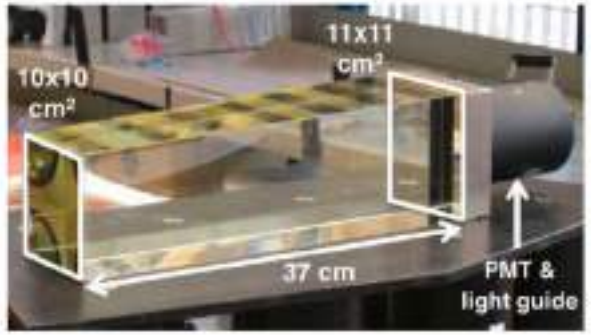

→ LED pulser + 2nd LG block installation before Run IV:

- LED pulser Tektronix AFG3101
- Independent trigger integrated in DAQ
- 2nd LG block out of beam acceptance (LED only)
- Run-per-run LG response renormalized to **non-fired-block**
  - Monitor and calibration
  - Reference for Light Yield response
- System continuously operated **only during Scan 2**
- +3 independent measurements: Target, padMMe, TMM

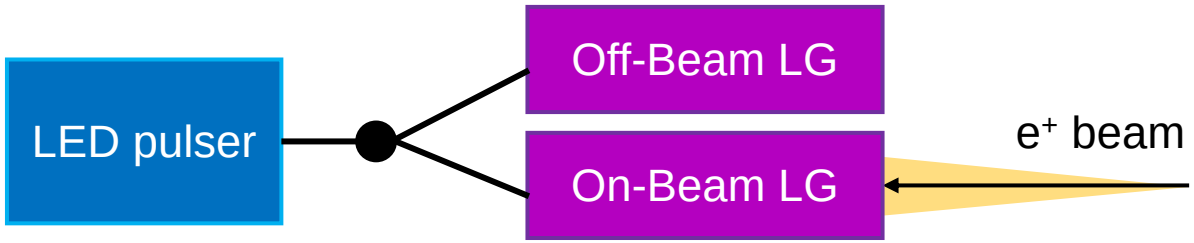

LED independent Trigger $\mathcal{O}$(2-4 Hz)

Conclusions

Run III:

- Overall systematic uncertainty below 0.9% achieved for the entire Run III dataset
- No statistically significant X_{17} signal observed largest fluctuation at $M_X = 16.90$ MeV (**2.5σ** local - **1.8σ** global)
  - Results interpreted with a **frequentist CLs** procedure to set **upper limits** (vector-boson hypothesis).

Run IV:

- **36 energy scan points** ($\geq 2\times10^{10}$ PoT each) equally separated by 0.75 MeV in the around resonance region
  - Signal yield increased by a factor of ~ 2.5 wrt Run III (luminosity+acceptance)
- Ongoing developments:
  - Use of tracks information
  - Redundant beam parameter measurements
  - Finalization of event reconstruction algorithm

Improve sensitivity (higher statistics and better control of systematics) aiming at a factor of **2 error reduction**

How to close the X_{17} parameter space?

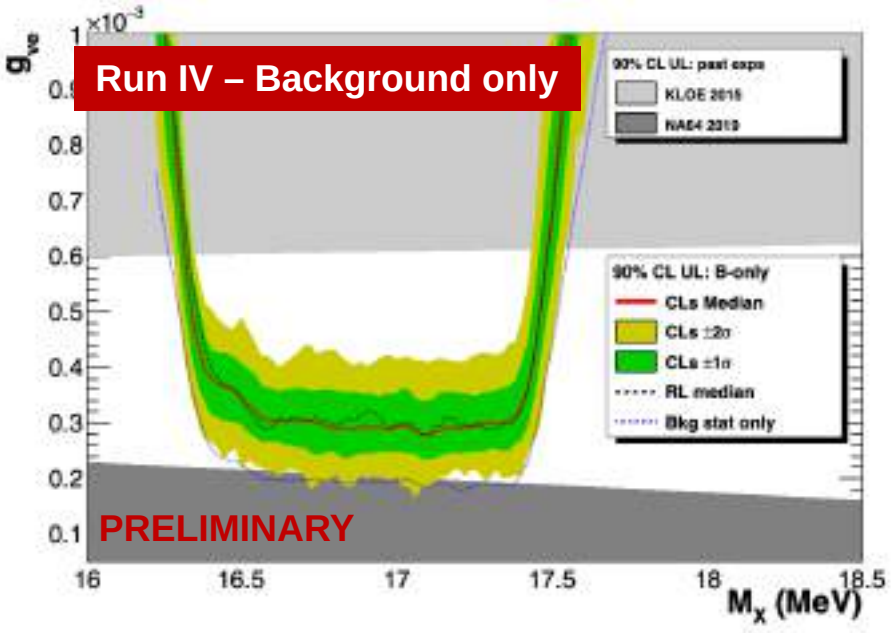

Incremental improvements using present beam setup:

- Tune target material and thickness to reduce spread induced by atomic electron motion and maximise Yield/BIB (Tag&Probe + MM occupancy)
  - About ×2 Signal/Bkg
- Further tune tracker+ECal position to increase acceptance (~30%)
- Use non-zero PADME magnetic field (**Beam test scheduled**)
  - A minimum induction field (~50 G), only to measure the charge of the particle in the final state → access to angular dependence
    - Systematic improvement on normalization
  - A stronger field (~150 G) providing adequate measurements of particle momenta → access to invariant mass (**new detector needed**)
    - Up to ×5 Signal/Bkg @ $\frac{\sigma_p}{p} \simeq 10^{-3}$

Upgrade of the beam setup → See next talk (P. Valente)

Back-up slides

Other experiments in the race

Recent result from MEG II, arXiv:2411.07994 still to be published

- Measurement on ^{7}Li target to reproduce ^{8}Be ATOMKI
  → no signal found
- ULs on $\frac{\Gamma\left(^{8}Be^{*}\rightarrow {}^{8}Be\, X_{17}(ee)\right)}{\Gamma\left(^{8}Be^{*}\rightarrow {}^{8}Be\,\gamma\right)}$ for 17.6 and 18.1 MeV transitions

MEG II result compatible at 1.5σ with the **ATOMKI combination** $M_X = 16.85(4)$ MeV [Barducci, et al. , JHEP 04 (2025) 035]

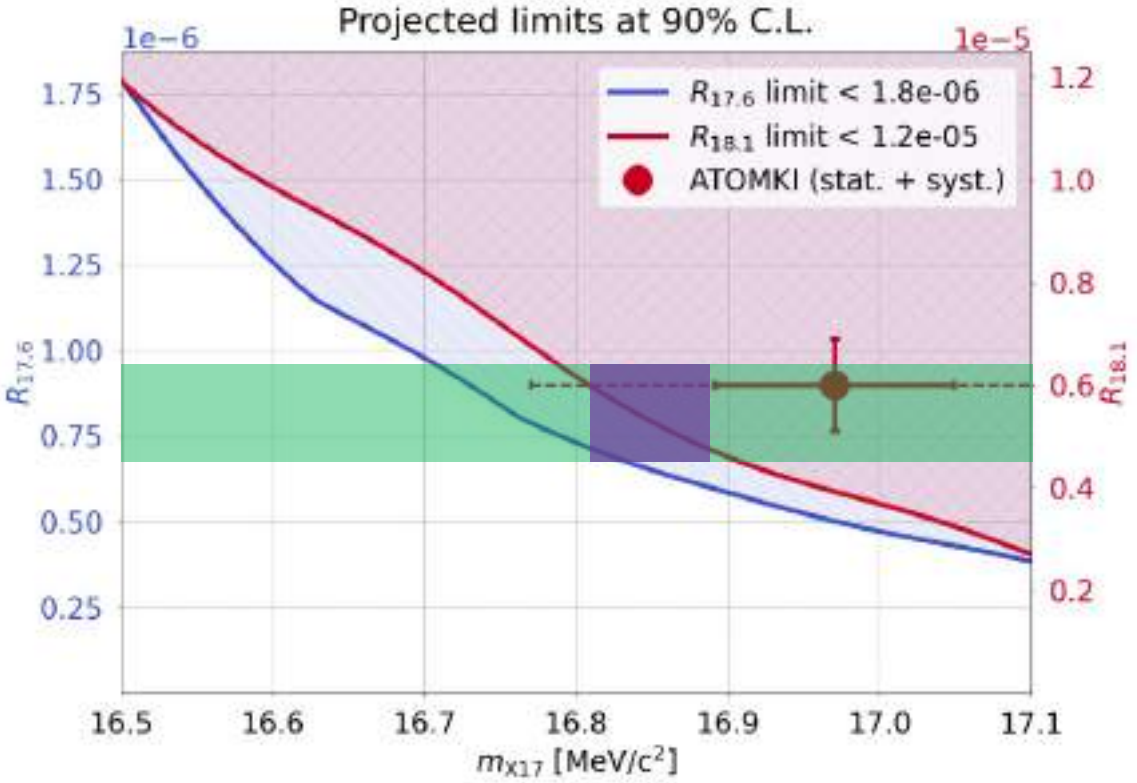

Further attempts to verify:

AN2000 facility @INFN-LNL [data taking ongoing]

n_TOF EAR2 neutron line @CERN [2025 proposal]

Tandem accelerator @Montreal [JPC Ser. 2391 (2022) 012008]

Van de Graaf accelerator @IEAP Prague [NIM. A 1047 (2023) 167858]

PADME facility

- Positrons from the DaΦNE LINAC up to 550 MeV, $\mathcal{O}(0.25\%)$ energy spread
- Repetition rate up to $49\ Hz$, macro bunches of up to 300 ns duration
- Intensity must be limited below $3\times10^4 PoT/spill$ against pile-up
- Emittance $1\ \mathrm{mm}\times1.5\ \mathrm{mrad}$ @PADME

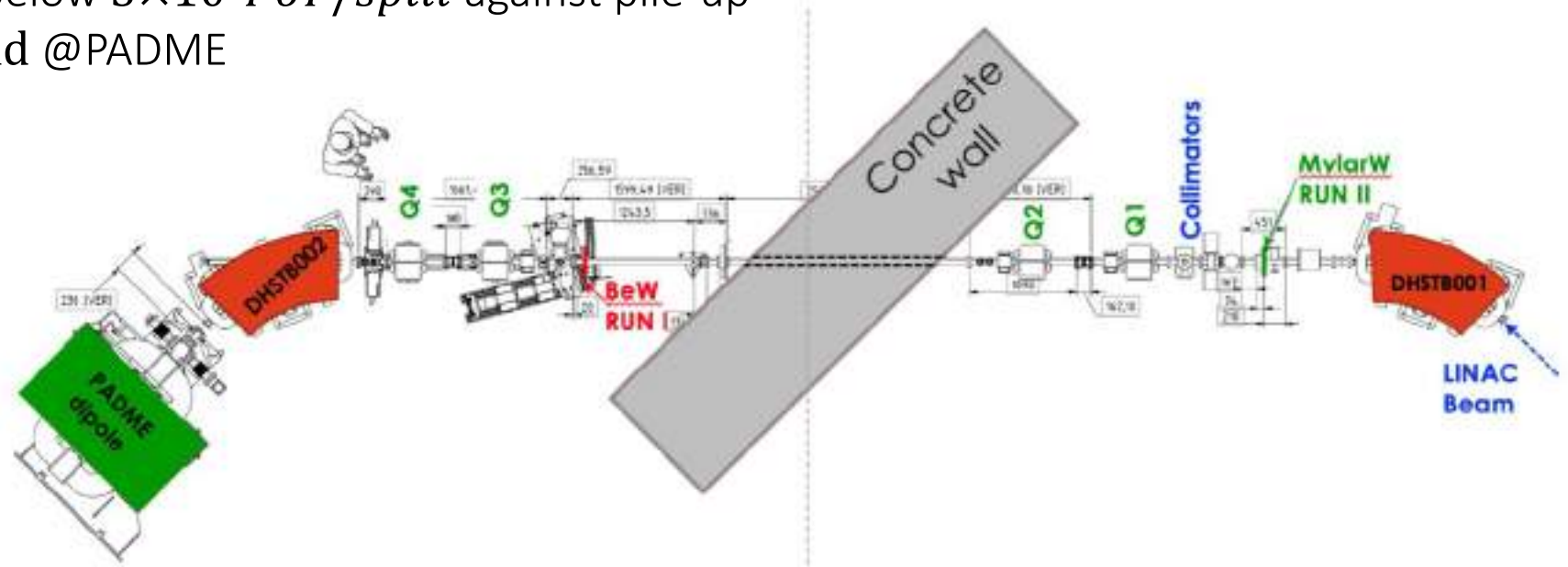

Past operations:

- Run I (2019): e^- primary, target, e^+ selection, $250\ \mu\mathrm{m}\ Be$ vacuum separation
- Run II (2019-20): e^+ primary beam, $125\ \mu\mathrm{m}$ Mylar™ vacuum separation, 28000 $PoT/bunch$
- Run III (end of 2022):dipole magnet off, $\sim 3000\ PoT/bunch$, scan $\sqrt{s}$ around ~ 17 MeV
- Run IV (2025): same conditions as Run III

Run III beam condition determination

Positron beam energy selected using the last 2 BTF dipole magnets: **DHSTB001** and **DHSTB002**

- e^+ momentum: $p\,[\mathrm{MeV}] = 0.05513 \times B[\mathrm{G}]$
- 2 possible magnet field determination:
  - Magnet current: $B[\mathrm{G}] = 28.42 \times I[\mathrm{A}] + 16.22$
  - Hall-probe direct reading

→ Systematic offset $\sim 20 - 30$ G leading to an absolute uncertainty in the $\sqrt{s}$ of about 20 keV

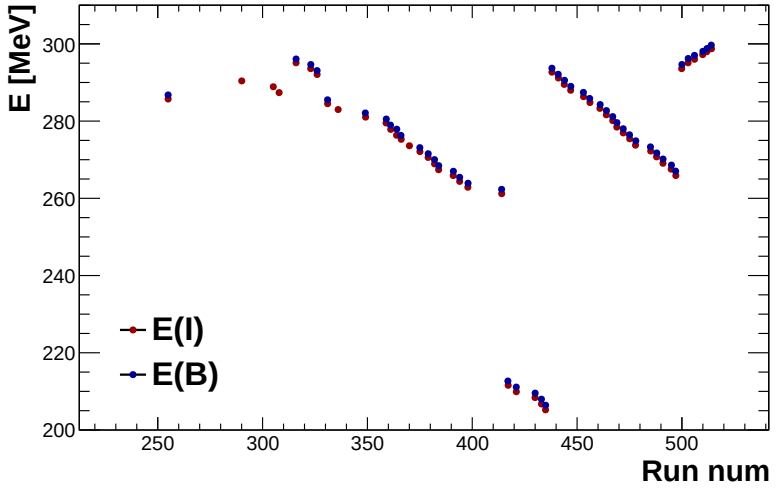

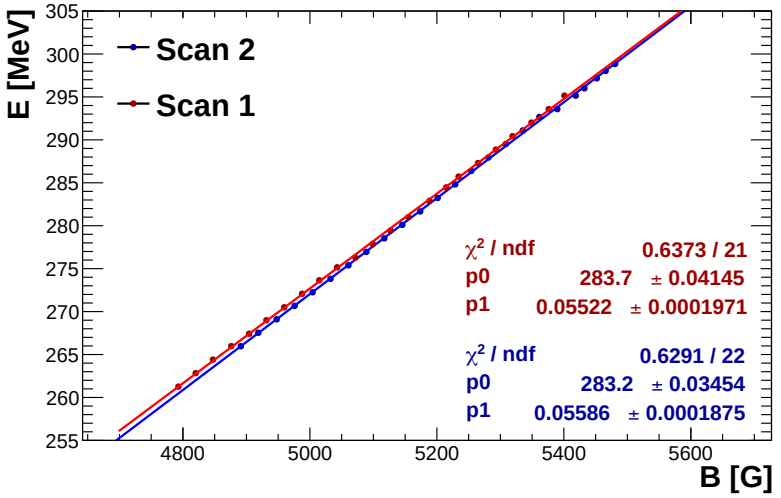

Nucl. Instrum. Meth. A515 (2003) 524

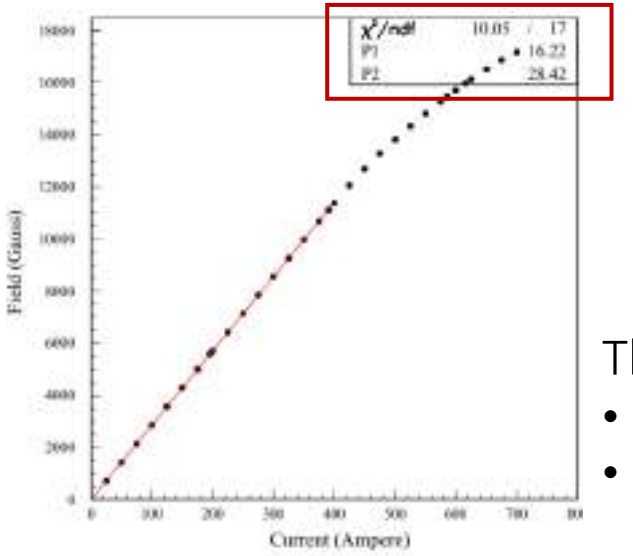

The *P1 parameter* depends on:

- Residual magnetization – variable during the data taking
- Position of the Hall probe

Run III beam condition determination

DHSTB001 introduces chromatic dispersion → correlation $\Delta\phi/\phi$ - $\Delta E/E$

- BTF beam line acts as an effective momentum spectrometer
  - $\left|\frac{\Delta E}{E}\right| = \frac{h}{2\rho} + \sqrt{2}\left(\frac{R_x}{L_1} + \frac{H}{2L_1}\right)$
- Expected value compared with MC beam-line simulations
  - Real SLTB5 aperture considered [M.Raggi et al, JHEP 09 (2022) 233](#)
  - Conservative configuration with SLTB5 open

Collimator	Symbol	Aperture [mm]
SLTB2	H	1.5
SLTB3	V	4.3
SLTB4	h	2.1
SLTB5	—	0.9

Last collimator before PADME

$\frac{\Delta E}{E} < 0.25\%$ for the entire Run III → subdominant once the atomic electron motion effect is introduced

[Nucl. Instrum. Meth. A515 (2003) 524](#)

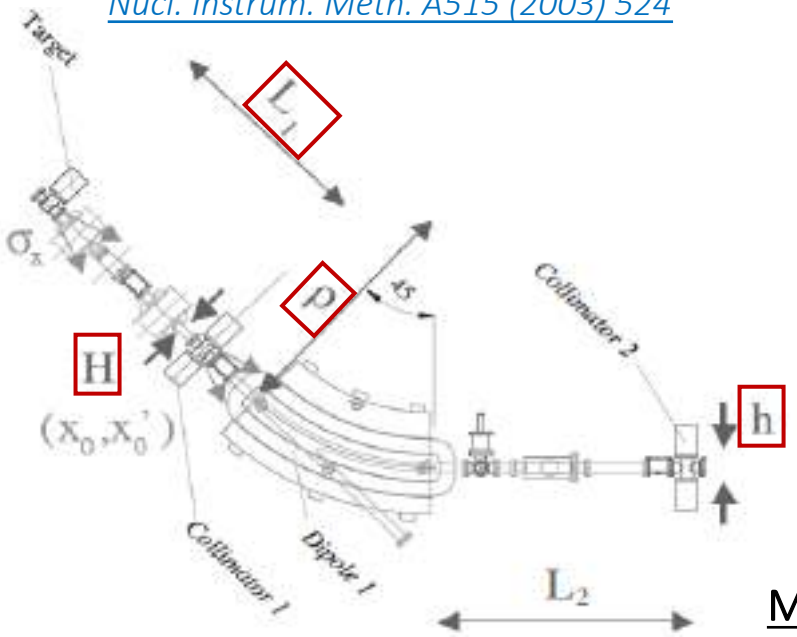

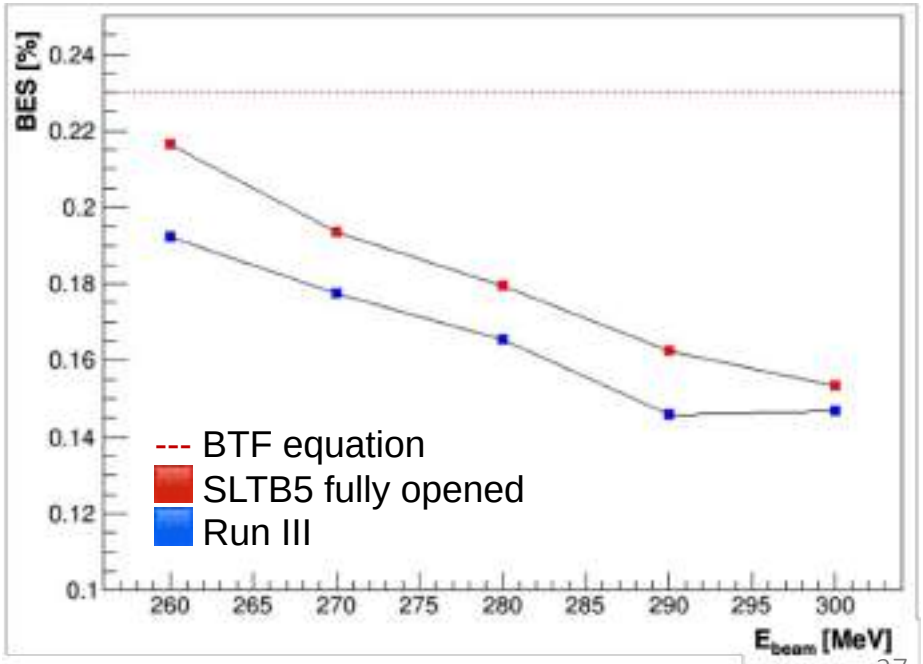

More on the beam line

BTF beam line and energy selection

TimePix3 pictures

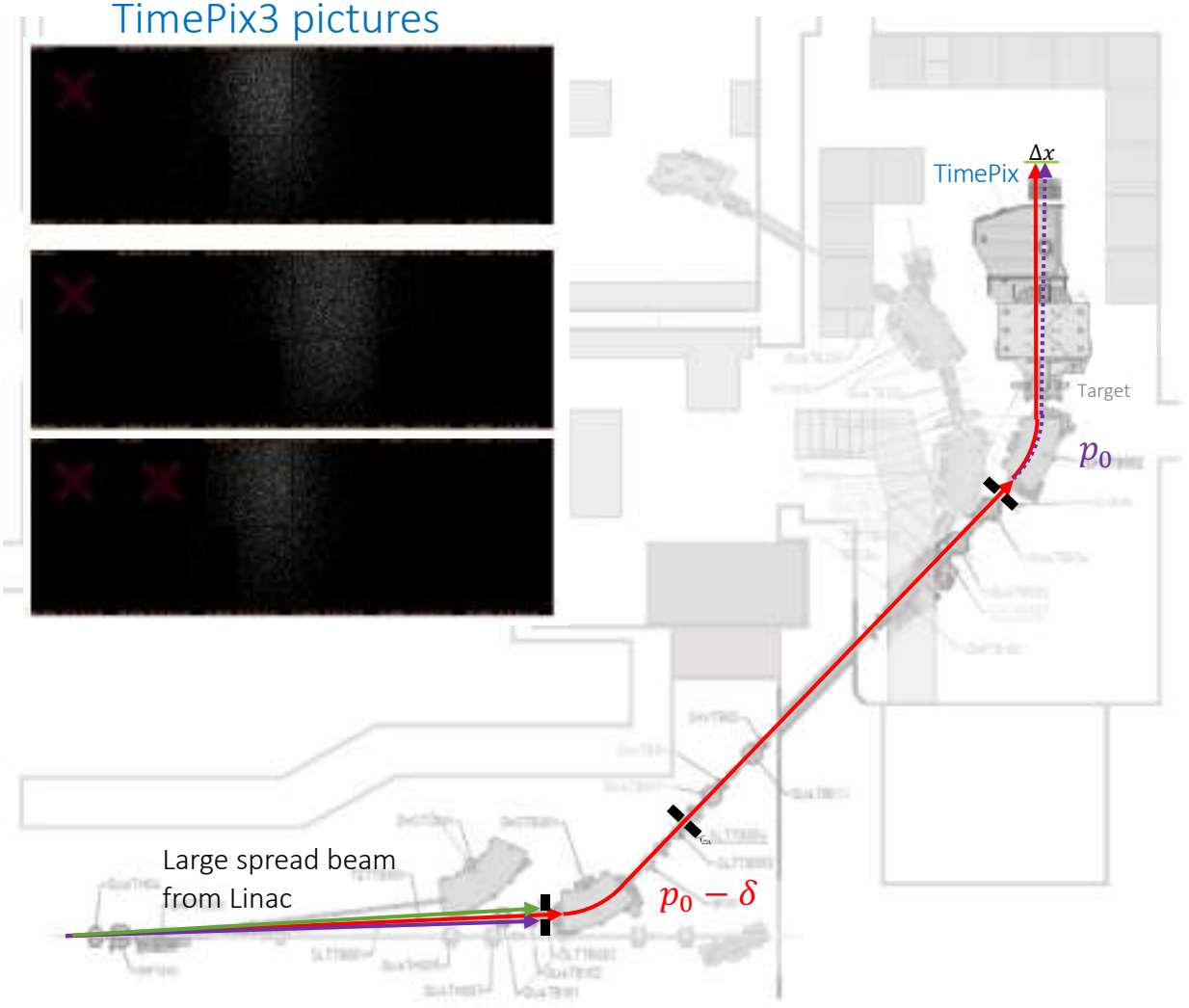

In a spectrometer line the horizontal position of a particle with momentum $p = p_0(1+\delta)$ with $\delta = \sigma_p/p_0$, will be offset by $\Delta x = D_x\delta$, where D_x is the dispersion function; $D_x \approx L\varphi$ (L is the arm length and φ the deflection angle)

The beam spot size is given by: $\sigma_x = \sqrt{\varepsilon\beta + \left(\frac{D_x\sigma_p}{p}\right)^2}$

If the geometric beam size in absence of dispersion can be neglected, $\sqrt{\varepsilon\beta} \ll \frac{D_x\sigma_p}{p}$, we can get the spread from:

$$\frac{\sigma_p}{p} \approx 1/D_x \cdot \sigma_x$$

From a **run without PADME target** (otherwise Coulomb scattering would be not negligible) we estimate: $\frac{\sigma_p}{p} \approx 0.24\%$

Nucl. Instrum. Meth. A515 (2003) 524

- Can also be computed from collimators' gaps/distances

$$\left|\frac{\Delta E}{E}\right| = \frac{h}{2\rho} + \sqrt{2}\left(\frac{R_x}{L_1} + \frac{H}{2L_1}\right) \cong \frac{h}{2\rho} + \sqrt{2}\frac{H}{L_1}$$

- With $H = h = 2$ mm we get 0.22%

N_2 selection cuts

Selection algorithm as independent as possible on beam and detector conditions:

- Selected a cluster pair with the following criteria
  - Maximum radius defined by ECal dimensions
  - Energy within the “two-cluster” kinematic range
  - Minimum radius within the “two-cluster” kinematic range → following the beam center conditions
  - Illumination clearly affected by material along the beam line (magnet bore) → Cut regions in φ
- Mutual cluster conditions:
  - ΔT (clu0-clu1) < 5 ns
  - ΔR (clu0-clu1) > 60 mm (Minimum 2CL difference)
  - $\boldsymbol{\phi_1 - \phi_2}$ vs $\boldsymbol{\theta_1 + \theta_2}$ cut in the center of mass frame isolates the signal

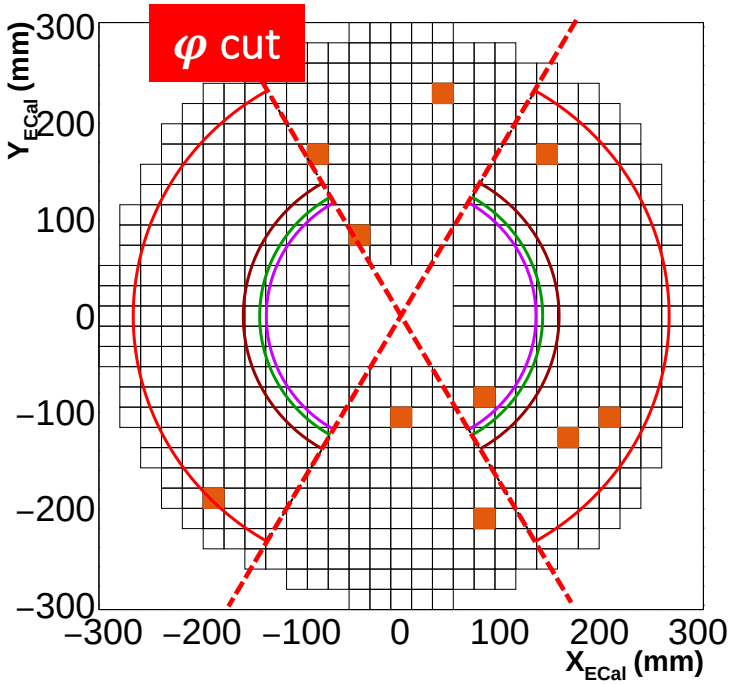

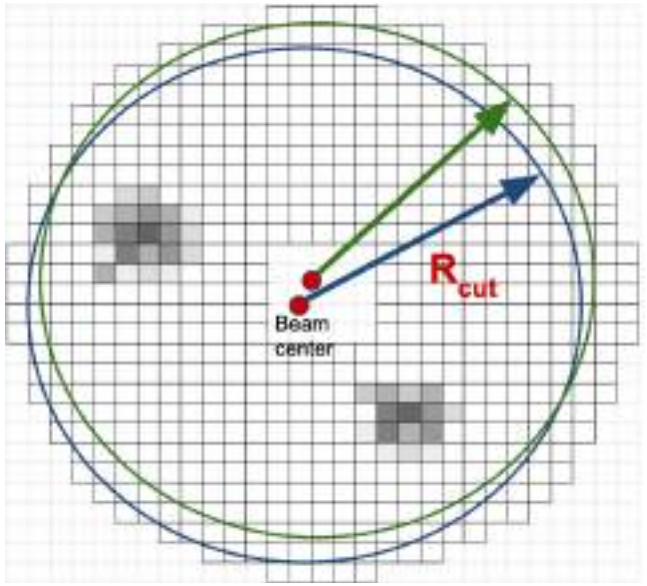

N_2 selection and Bremsstrahlung removal

- $\boldsymbol{\phi_1 - \phi_2}$ vs $\boldsymbol{\theta_1 + \theta_2}$ cut isolates the signal→ 3σ around the mean value
- 2 Clusters event surviving the whole set of cuts:
  - $E_1 + E_2 = E_{beam}$ as expected for a 2-body final state process
  - Time coincidence verified
- Flat beam bkg in $\boldsymbol{\phi_1 - \phi_2}$ → bkg level < 4%
- Bremsstrahlung tail in $\boldsymbol{\theta_1 + \theta_2}$ subtracted by using MC shape on the sideband

→ Statistical error: δN_2 ~0.6% up to 0.7%

→ Systematic uncertainty due to bkg subtraction: δN_2 ~ 0.3%

Source	Error on N_2 [%]
Statistics	~0.6
Background subtraction	0.3
Total	0.65

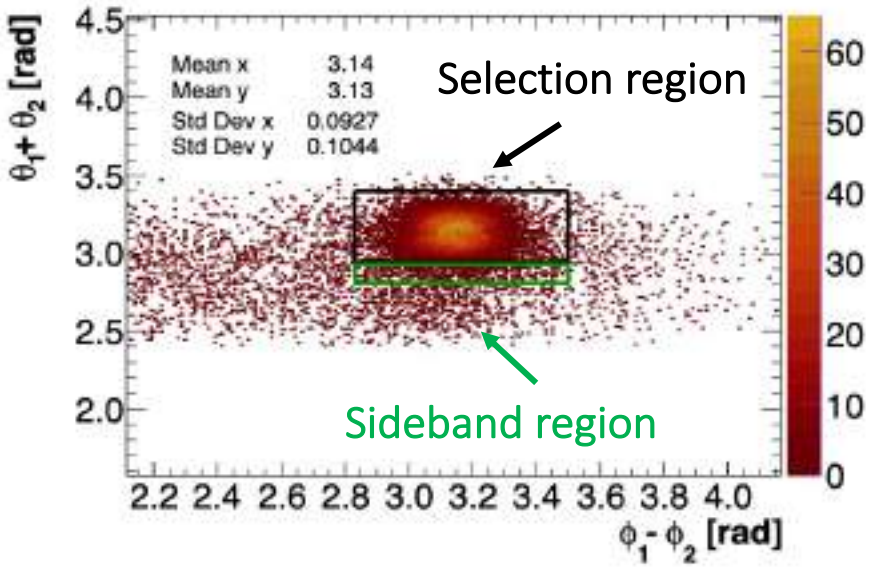

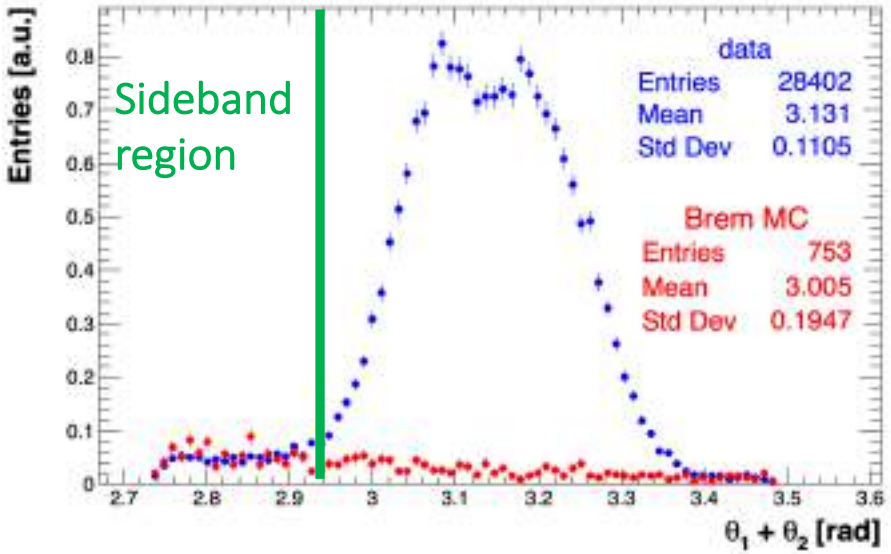

Shape of ee signal due to residual PADME magnetic field

→ Fully modelled using MC + detailed map

SM bkg B uncorrelated error budget

The expected background yield B is determined with MC + data-driven checks

Reconstruction efficiency:

- Data/MC efficiency with tag-and-probe technique
- bkg subtraction at tag level dominates the statistical-systematic error → $\delta B = 0.35\%$

The selection relies on the expected beam direction: spot measured at the target and the Center of Gravity (COG) of 2 body final states at ECal

- Systematic shifts in the COG position → acceptance systematic errors
- Largest effect in y due to acceptance limitations (magnet bore)
- Fractional variations range from 0.08% to 0.1% mm^{-1} for $\sqrt{s}$ = (16.4, 17.3) MeV

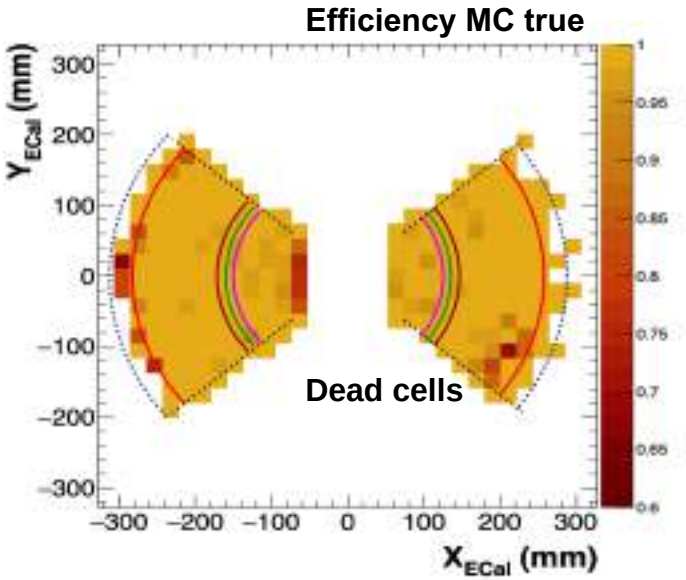

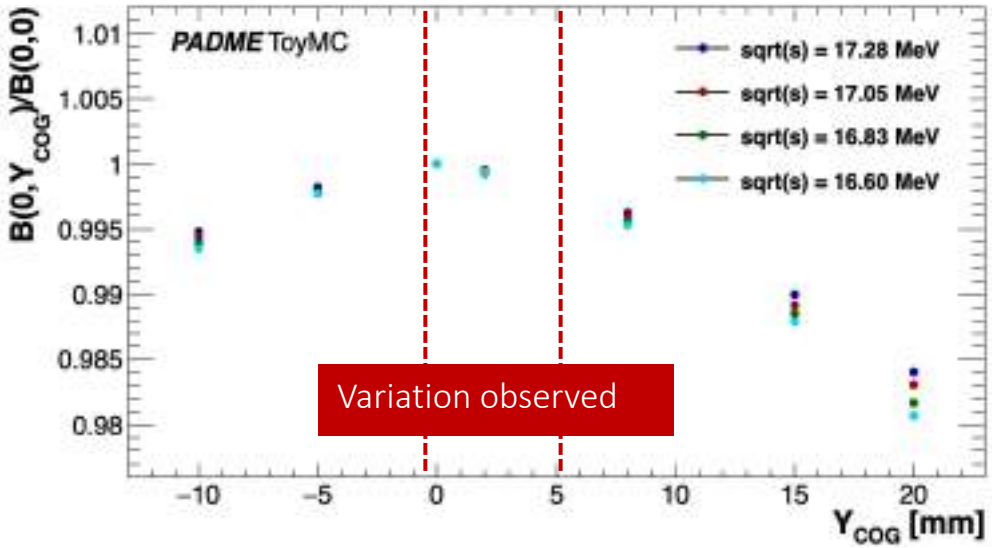

Source	Error on B [%]
MC statistics	0.40
Data/MC eff. (Tag&Probe)	0.35
Cut stability	0.04
Beam spot variations	0.05
Total	0.54

SM background B error budget – Run III

- Expected background B determined from MC, stat error per period: $\delta B \sim 4 \times 10^{-3}$
- Fit of B($\sqrt{s}$) with a straight line (only including statistical errors here)

Background curve slightly depend on the scan → Considered in alternative analysis (see later)

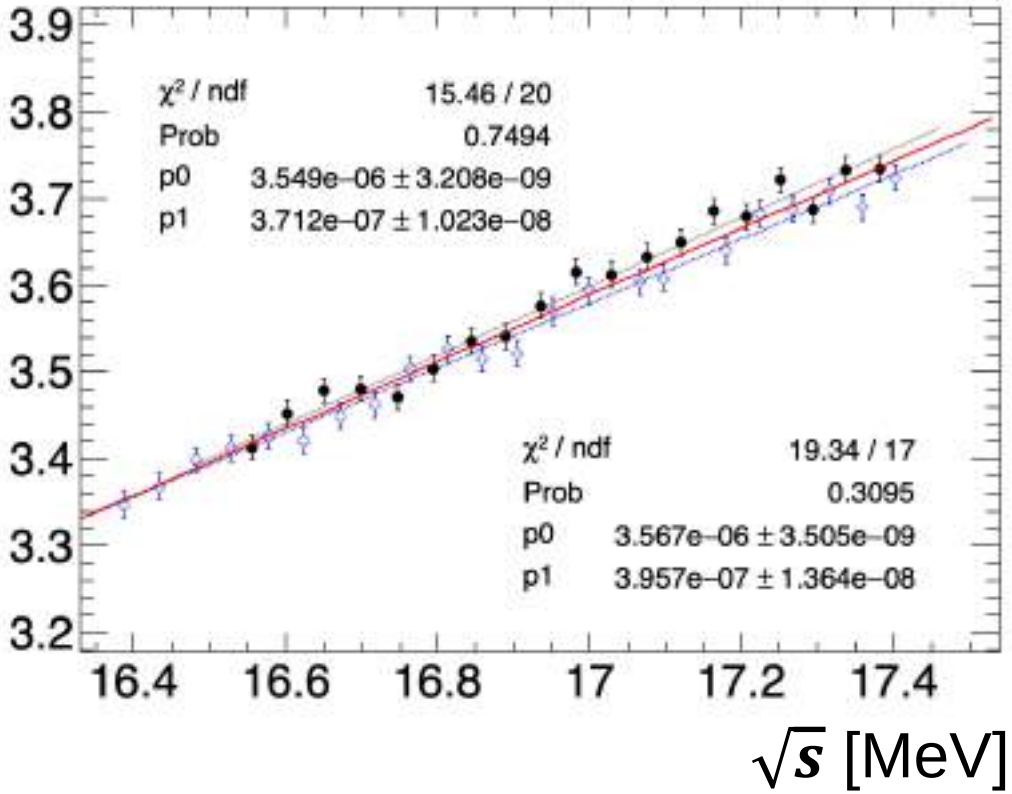

Fit mode	P0 [10^{-6}]	P1 [10^{-7} / MeV]	Corr	Fit prob
Only scan1	3.549(3)	3.71(10)	0.12	75%
Only scan2	3.567(4)	3.96(13)	-0.19	31%
All periods	3.558(2)	3.85(8)	-0.008	9%

Tag&Probe – reconstruction efficiency

Tag and probe technique, the method-induced bias is 2.3(2)% and stable along the data set

Data/MC method efficiency stable along the data set and at the few per mil

Efficiency Data/MC

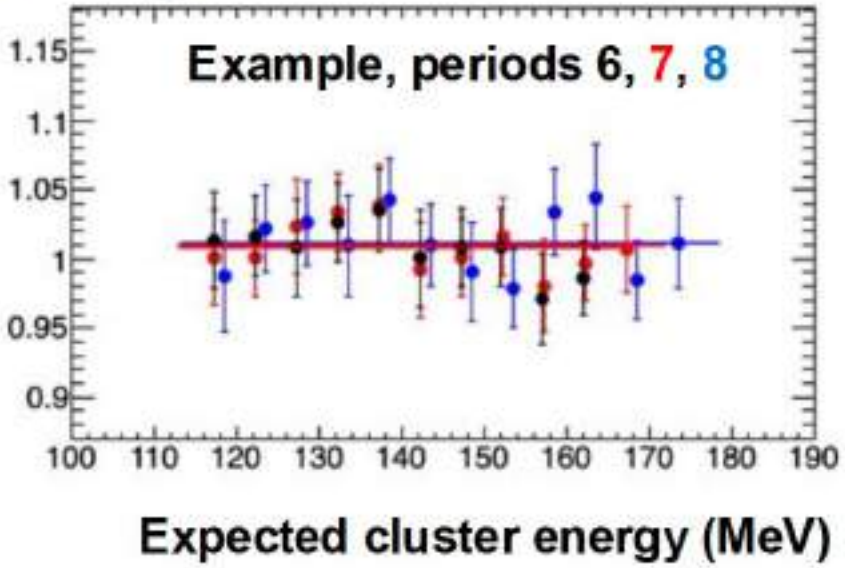

Efficiency <Method /MC true>

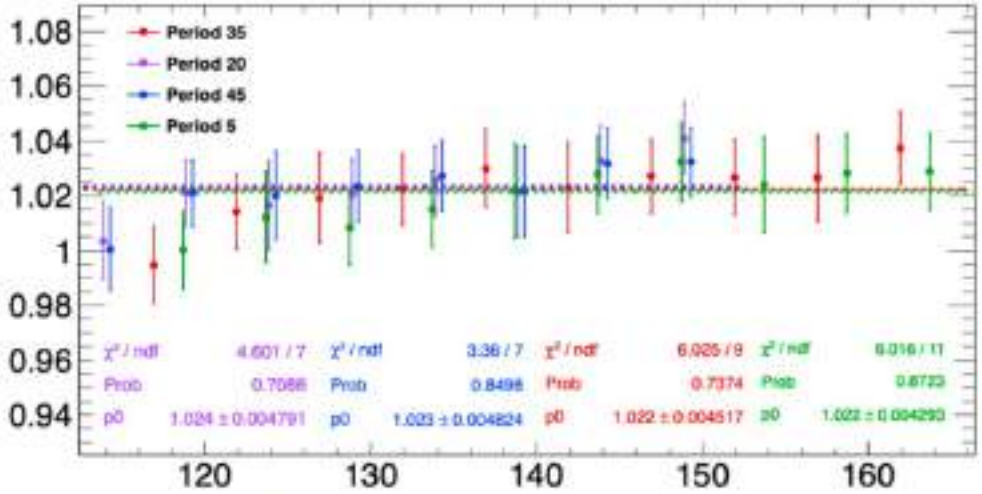

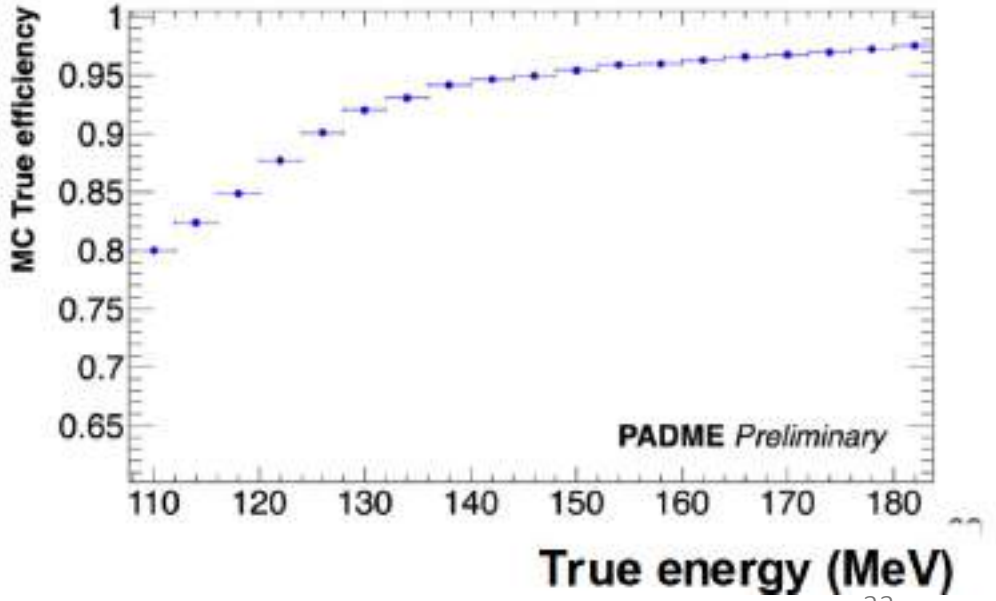

N_{PoT} error budget

Flux N_{PoT} determined using LG detector charge: $N_{PoT} = \frac{Q_{LG}}{Q_{1e^+,402\,[\mathrm{MeV}]}} \times \frac{402\ \mathrm{MeV}}{E_{beam}\,[\mathrm{MeV}]}$ → common systematic error @2%

2 main effects: **radiation induced loss** + **energy loss in passive material**

- Run III radiation dose ~ 2.5 krad → transparency changes for O(krad)
  - Estimated from 3 flux proxy observables: $Q_{target\text{-}x}$, $\langle E_{ECal} \rangle$, period multiplets
  - LG yield decreases with relative PoT slope of 0.097(7) → Slope error included δN_{PoT}= 0.35% (after correction applied)
  - Constant term uncertainty of δN_{PoT}=0.3% added as scale error
- Loss due to beam movements during the whole Run III → passive material crossing
  - Checked against data of October test beam + MC simulation → systematic correlated error δN_{PoT}=0.5%

Uncorrelated systematic errors on N_{PoT}

Source	Error on N_{POT} [%]
Statistics, ped subtraction	negligible
Energy scale from BES	0.3
Rad. induced loss, slope	Variable, ~0.35
Total	0.45

Common systematic errors on N_{PoT}

Source	Common error on N_{POT} [%]
pC / MeV (JHEP 08 (2024) 121)	2.0
Energy loss, data/MC	0.5
Rad. induced loss, const. term	0.3
Total	2.1

PADME beam-catcher calorimeter

The main detector for the flux determination [JHEP 08 (2024) 121]:

- SF57 block, reused from OPAL, tested for the NA62 LAV detector [JINST 12 (2017) 05, P05025]
- Several testing campaigns
  - A few positrons
  - O(2000) PoT - cross-calibration with the BTF FitPix

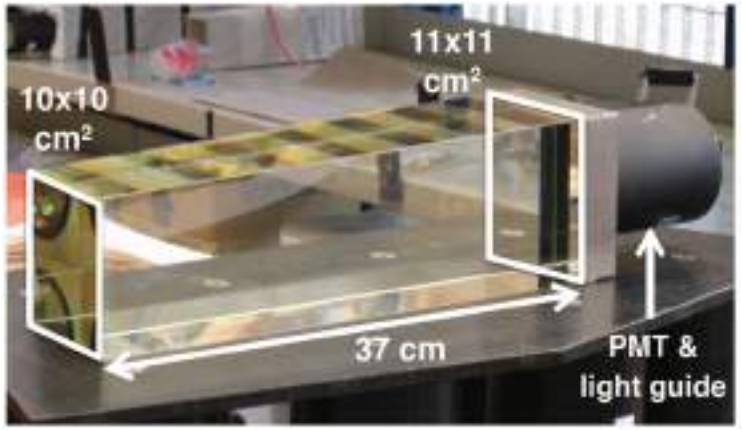

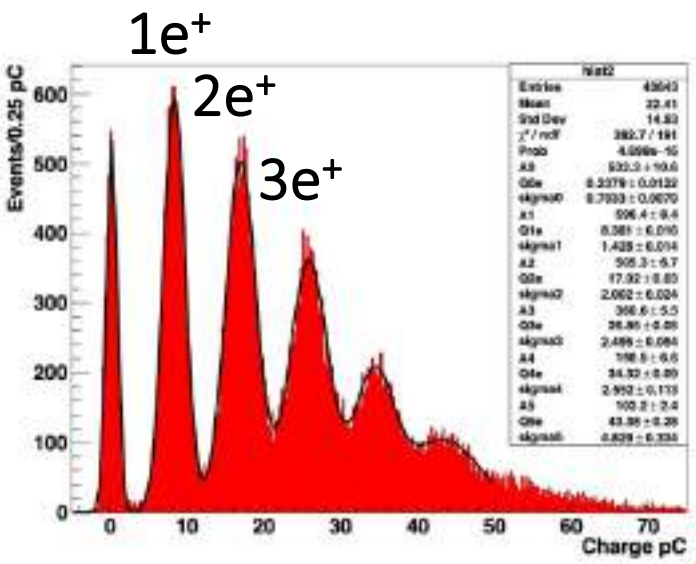

Figure 16. Single particle charge spectrum.

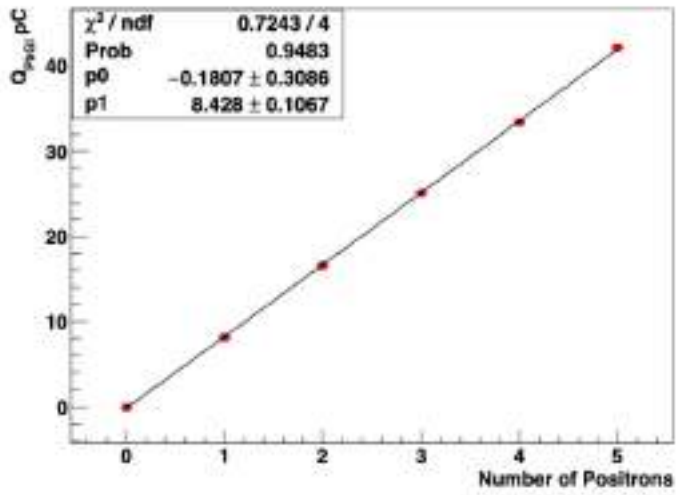

Figure 17. Fit to the single particle response.

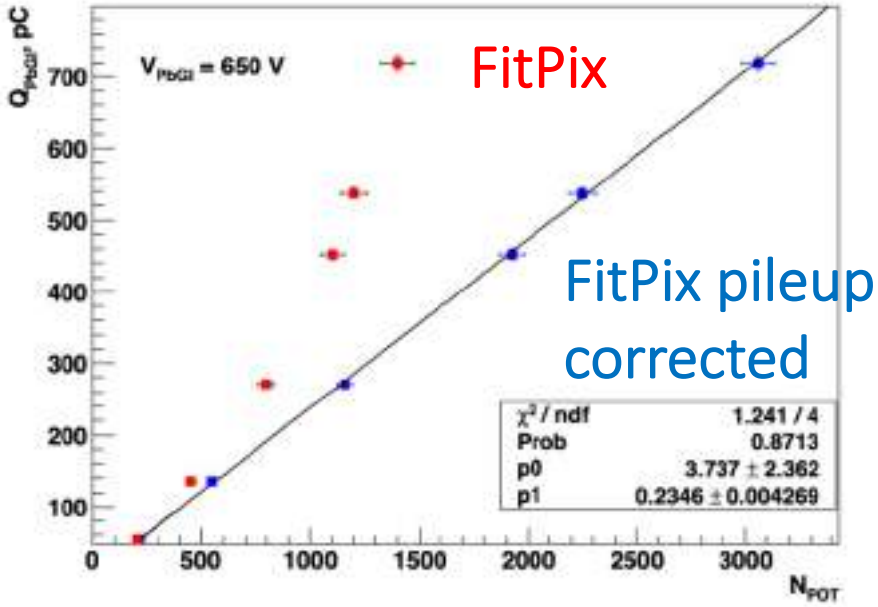

Energy Loss, Data/MC

- New Timepix geometry in PadmeMC to consider passive material (Cu)
- Using the Timepix beam spot it is possible to replicate the loss due to the copper also in Run 3
- Beam spot is not available for all the periods → we used the COG instead considering the Timepix-ECAL offsets and the intrinsic difference in resolution

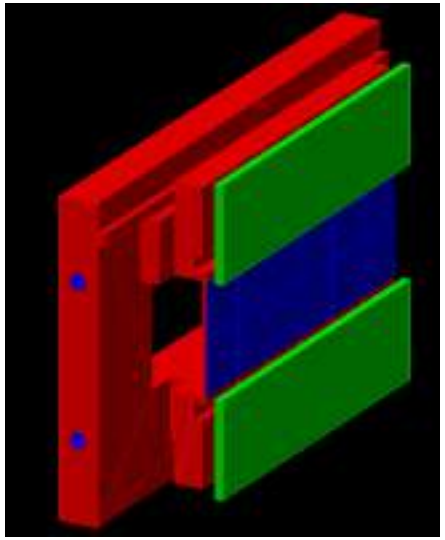

MC inputs

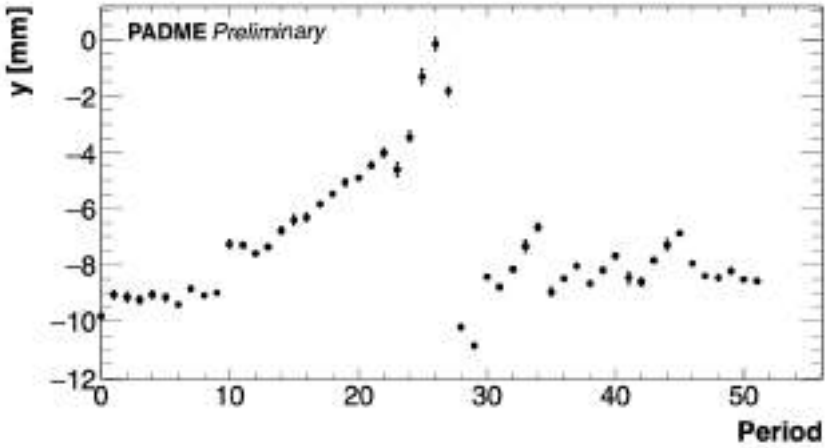

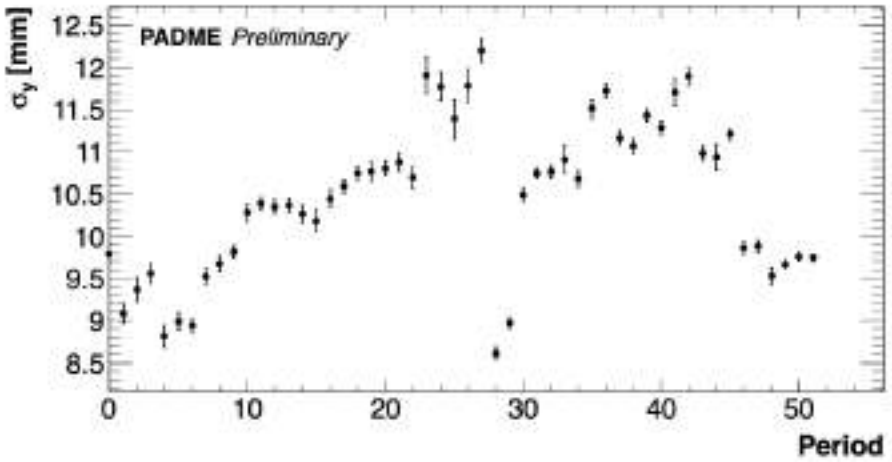

Relative leakage correction

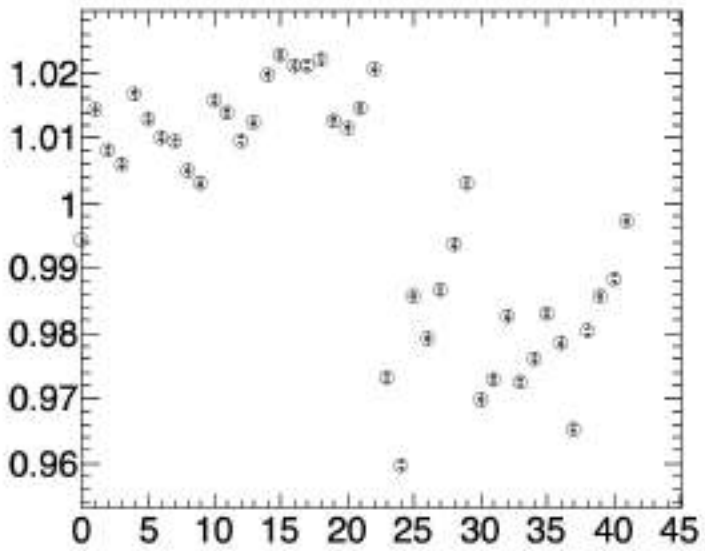

Energy Loss, Data/MC

How much do we trust the correction?

- Starting from october test beam data we tried to replicate the Y scan with PadmeMC
- Good data/MC agreement in the region where Run3 beam scanned
- **1.2% overall scale correction** (to address the Data/MC difference) **with a 0.5% error**

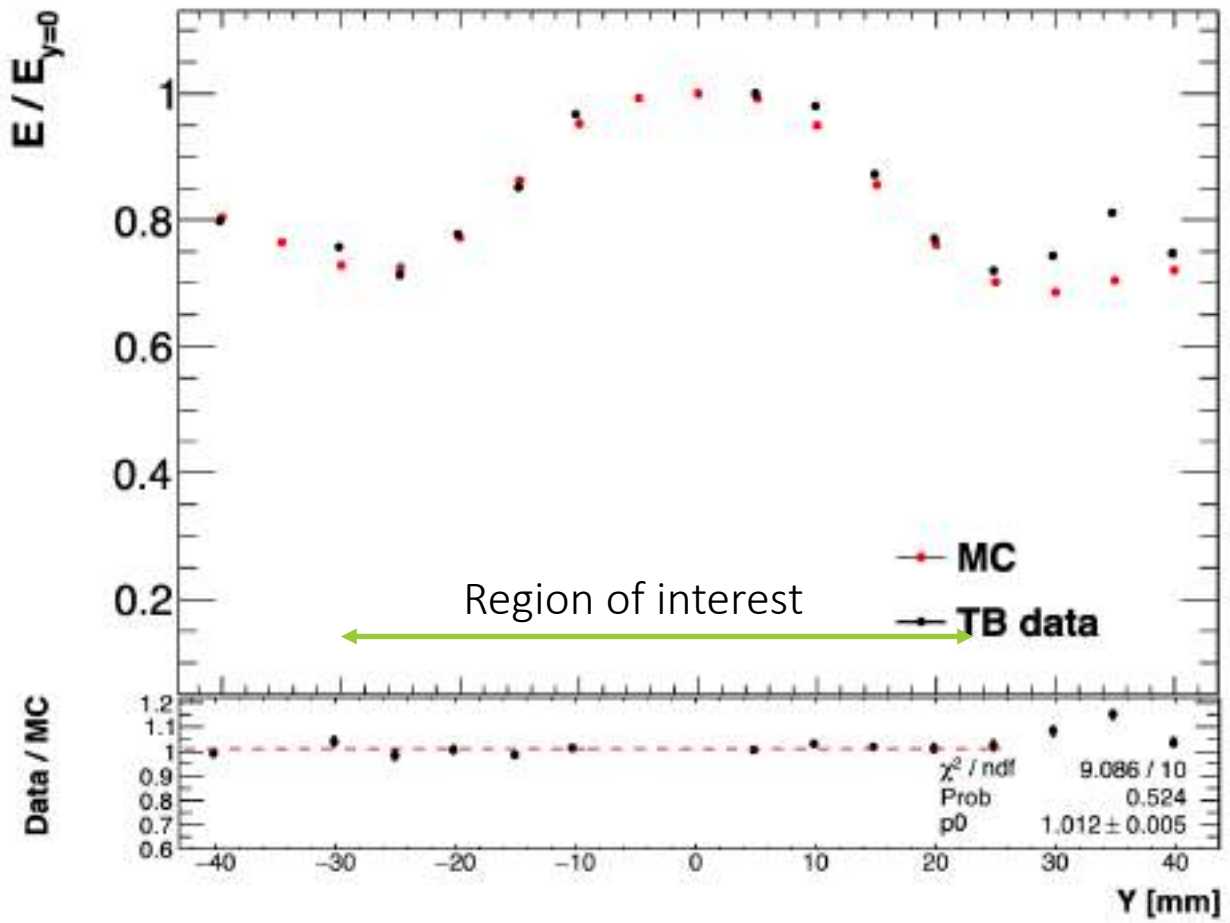

Radiation loss → E_{hit}/N_{PoT}

- First proof of loss of LY:
  - By looking at the ratio between the total energy per bunch in ECAL and the NPoT an increasing slope is visible → order 10%
  - Notice that EHit is particularly sensible to the beam spot variation (beam e^+ might enter) hence is prone to significant jumps between periods

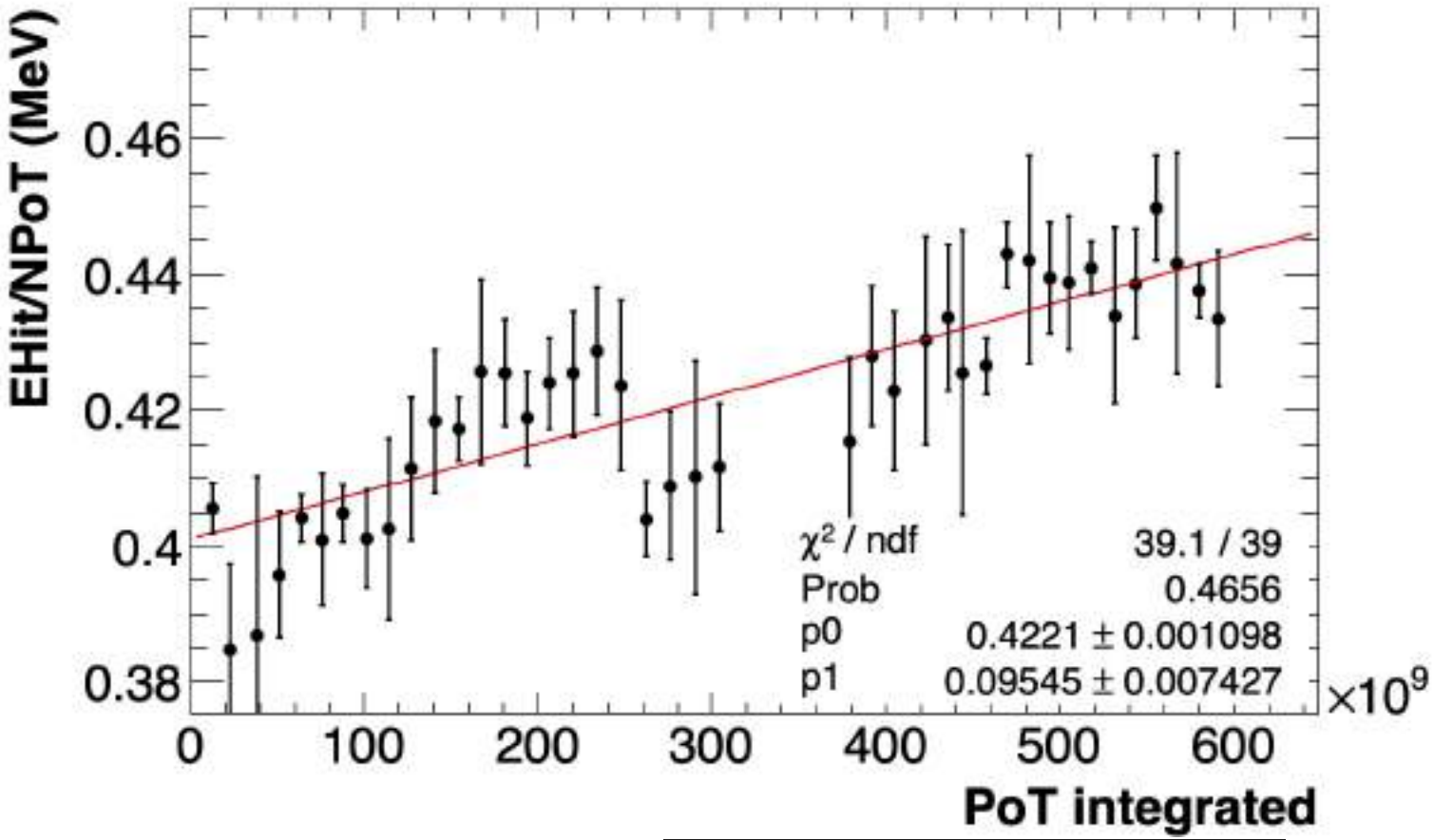

Correlation matrix

	0	1
0	1	0.04257
1	0.04257	1

Radiation loss → $Q_{X\text{-}Tar}/Q_{LG}$

- Second proof of loss of LY:
  - Target X strips are way more sensible than Y → can be used for quantitative checks
  - Shows an increasing slope → order 10% also here
  - During scan 1 (fitted) there were no “no target runs” hence the Qx response is reliable just in that part of Run 3
- **Conclusion:** use the weighted mean of the two proofs as Integrated PoT correction → 0.0967 +/- 0.0068

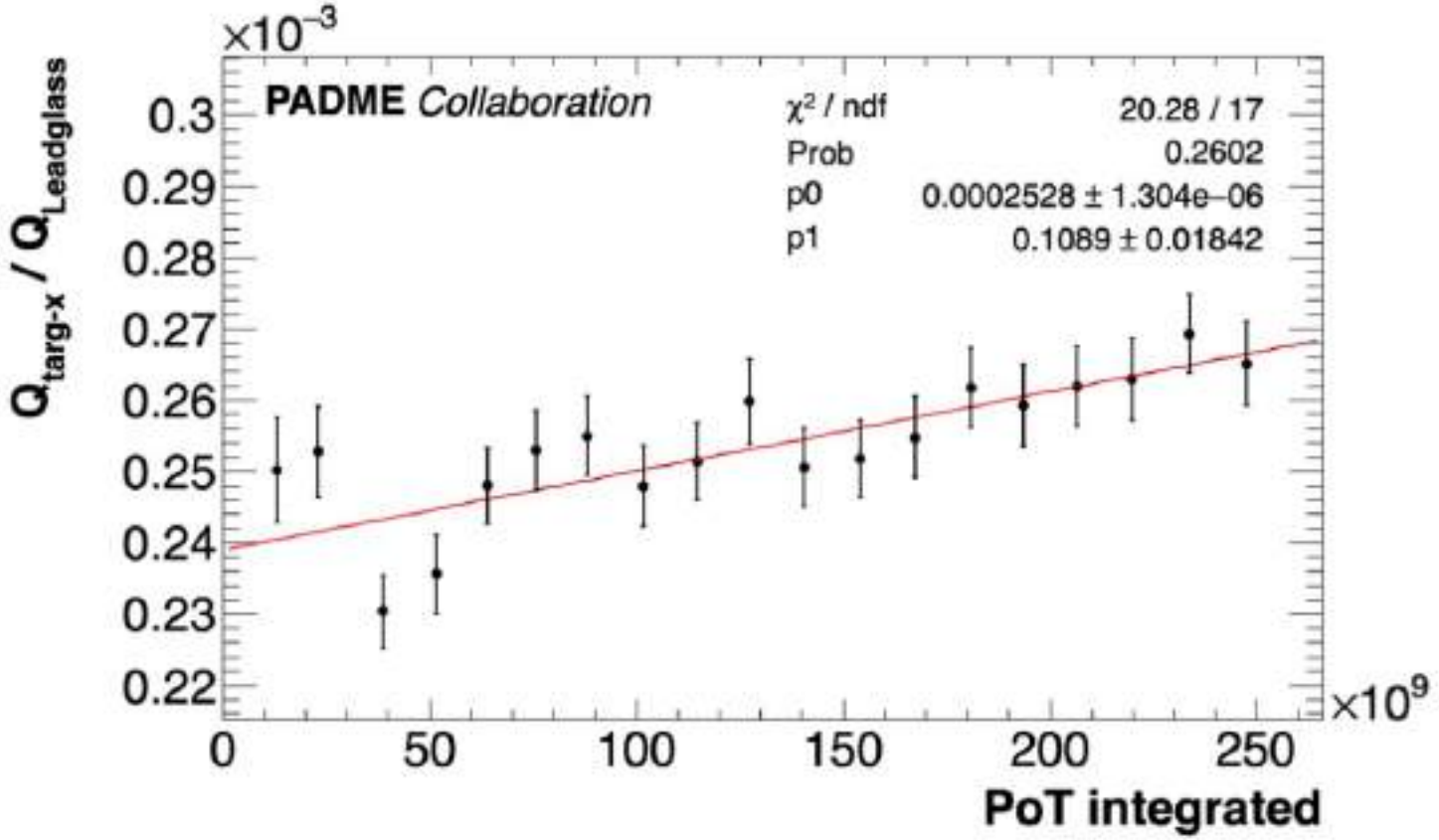

Correlation matrix

	0	1
0	1	0.4282
1	0.4282	1

Possible scale effects – K(s)

Radiative corrections evaluated using **BabaYaga** → $e^+e^-(\gamma)$ and $\gamma\gamma(\gamma)$ (*Nucl. Phys. B 758 (2006) 227*, *Phys. Lett B 663 (2008) 209*)

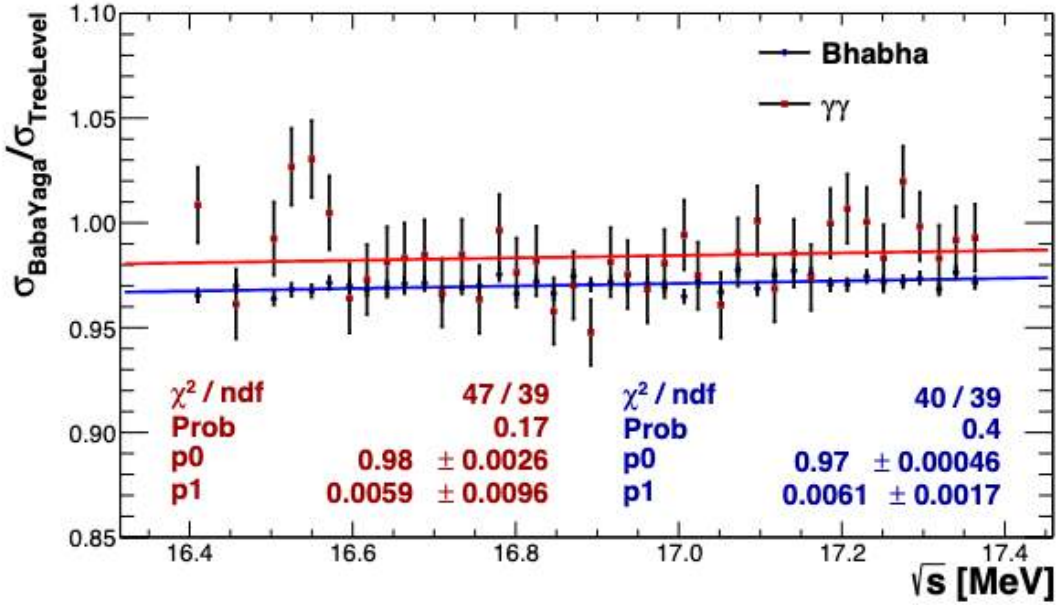

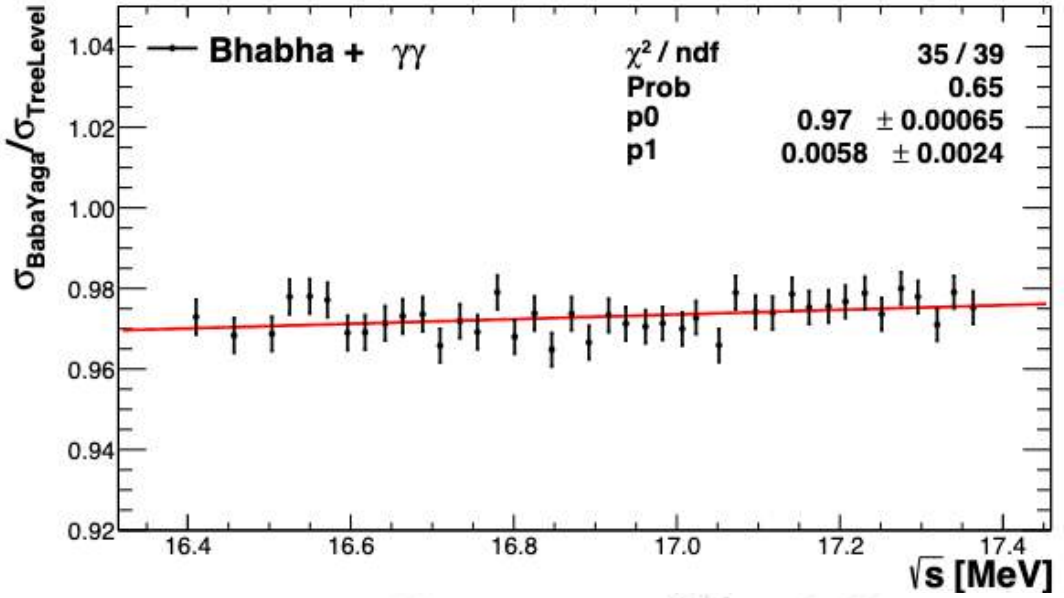

Possible **offset** → -2.8% @ 16.92 MeV
Possible **slope** with $\sqrt{s}$ → $-0.6(6)\%$ MeV^{-1}

The scaling with the below resonance is affected by a $-1.5(1.5)\%$ shift because of radiative correction, but the expected total error covers for it: 1.5%(B) + 2.1% (N_{PoT}) = 2.8%

Insertion of Babayaga-generated events in the MC (up to 10 γ's)
→ **no effect on ε(s)**

$K(s)$, constant term

Source	Uncertainty (%)
Lead-glass calibration	2.0
Absolute B yield	1.8
Energy-loss correction to N_{PoT}	0.5
Radiation-induced correction to N_{PoT}	0.3
Total	2.8

$K(s)$, $\sqrt{s}$-slope

Source	Expected value (%/MeV)
Radiative corrections	$-0.6 \pm 0.2 \pm 0.6$
Total	-0.6 ± 0.6

The atomic electron motion

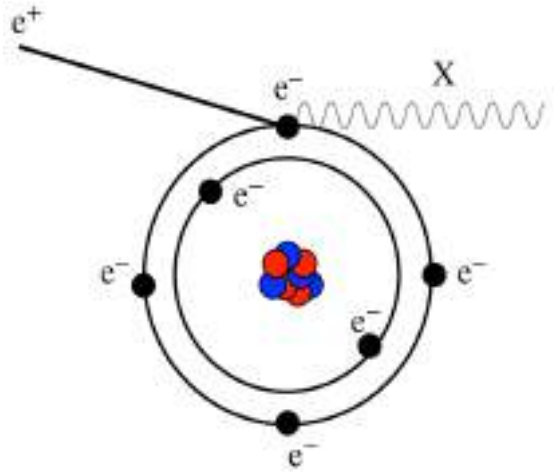

$$d\sigma = \frac{d^3p_X}{(2\pi)^3}\int \frac{d^3k_A}{(2\pi)^3}\frac{(2\pi)^4}{8E_XE_AE_B|v_A - v_B|}\boxed{n(\vec{k}_A)}|\mathcal{M}|^2\delta^4(k_A + p_B - p_X)$$

$\boxed{n(\vec{k}_A)}$

- **Theory**: use Slater Type Orbitals, hybridization, Hartree Fock computations for atomic carbon, …
- **Data**: obtain $n(\vec{k}_A)$ from data: Compton Profile, electron momentum distributions

Line shape modification

- Bound e^- momentum changes the e^+e^- invariant mass → Signal/Bkg worsens

$n(\vec{k}_A)$:

- Theory: calculate it using Hartree-Fock
- Data: X-ray determination of electron momentum density

X-Ray determination of the Electron Momentum Density in Diamond, Graphite and Carbon Black [*Phys. Rev. 176 (1968) 900*]

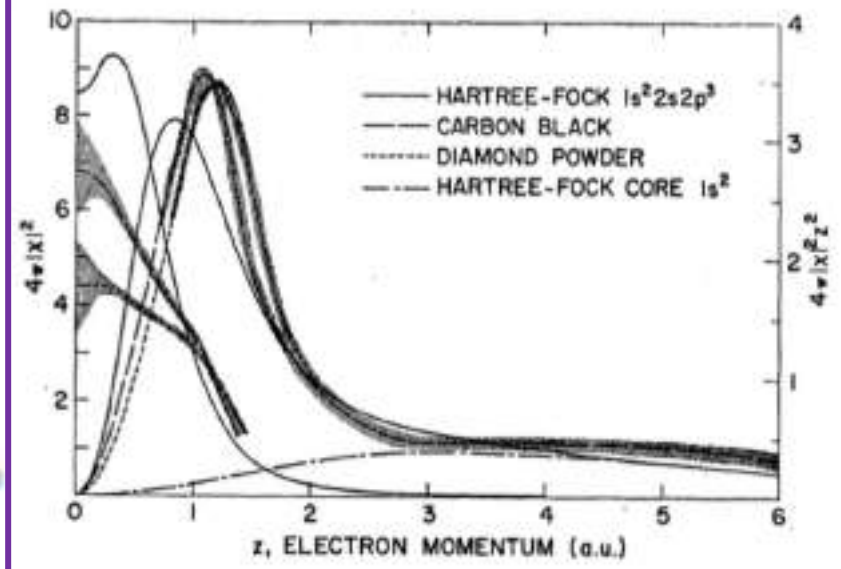

Theoretical Compton profile of diamond, boron nitride and carbon nitride [*Physica B 521 (2017) 361-364*]

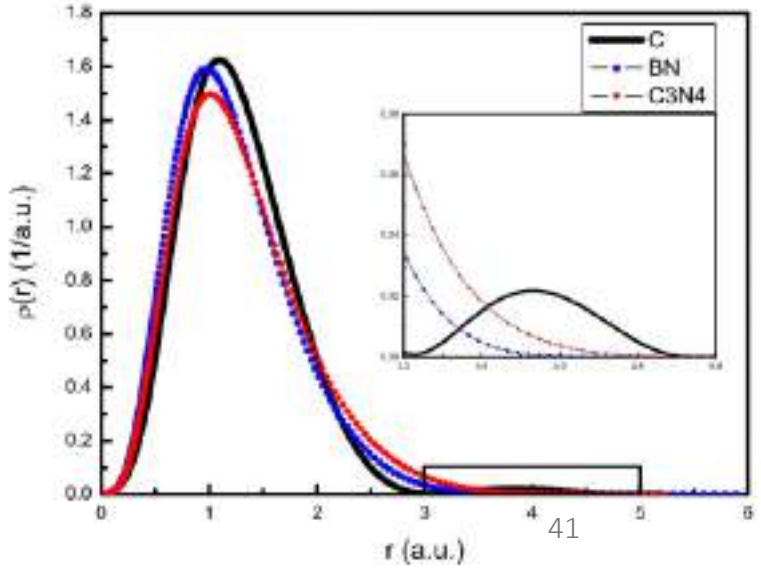

Phys. Rev. Lett. 132.26 (2024
EPJ Web Conf. 314 (2024)
Phys. Rev. Lett. 134.6 (2025)

Signal shape and ε/B

Electron motion inside the target changes significantly the resonance shape → not anymore just a gaussian with σ equal to the beam energy spread

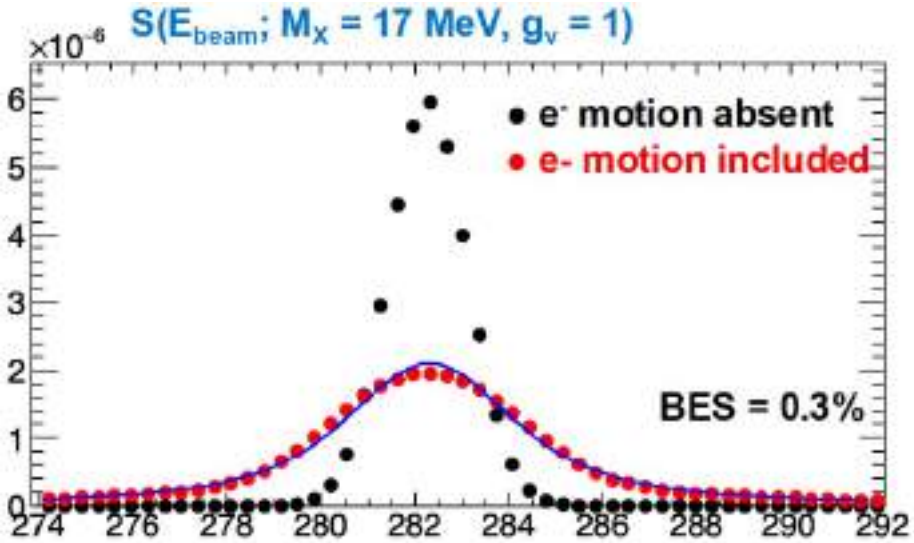

- Signal parametrized vs E_{beam} with a **Voigt** function:
  - Convolution of the gaussian BES with the Lorentzian
- Uncertainty in the curve parameters as nuisances:
  - **Lorentzian width** around the resonance energy: $1.72(4)$ MeV
  - **Relative BES**: $0.025(5)\%$
- Expected signal efficiency ***ε*** determined from MC:
  - Large cancellation of systematic errors if using ***ε*** /B
- Fit **ε(s)/B(s)** with a straight line → fit parameters as nuisances:
  - **Errors:** $\frac{\delta P0}{P0} \sim 0.1\%$, $\frac{\delta P1}{P1} = 3\%$, correlation = -2.5%

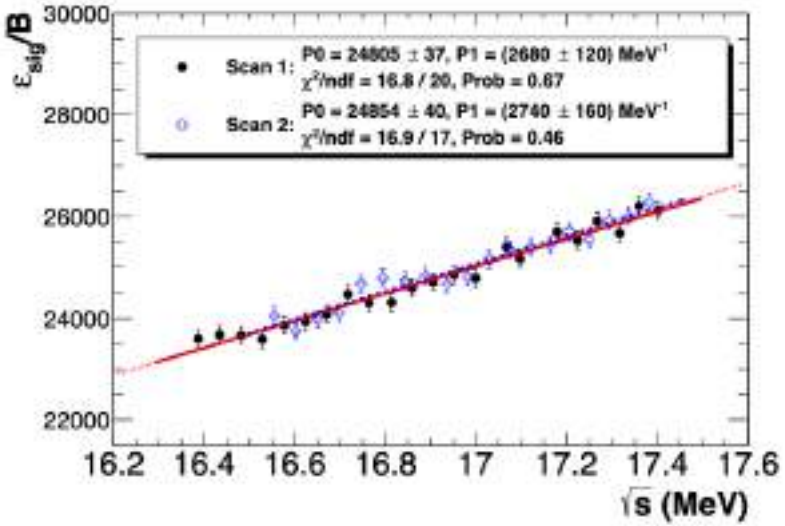

JHEP 11(2025), 007

Target waveforms

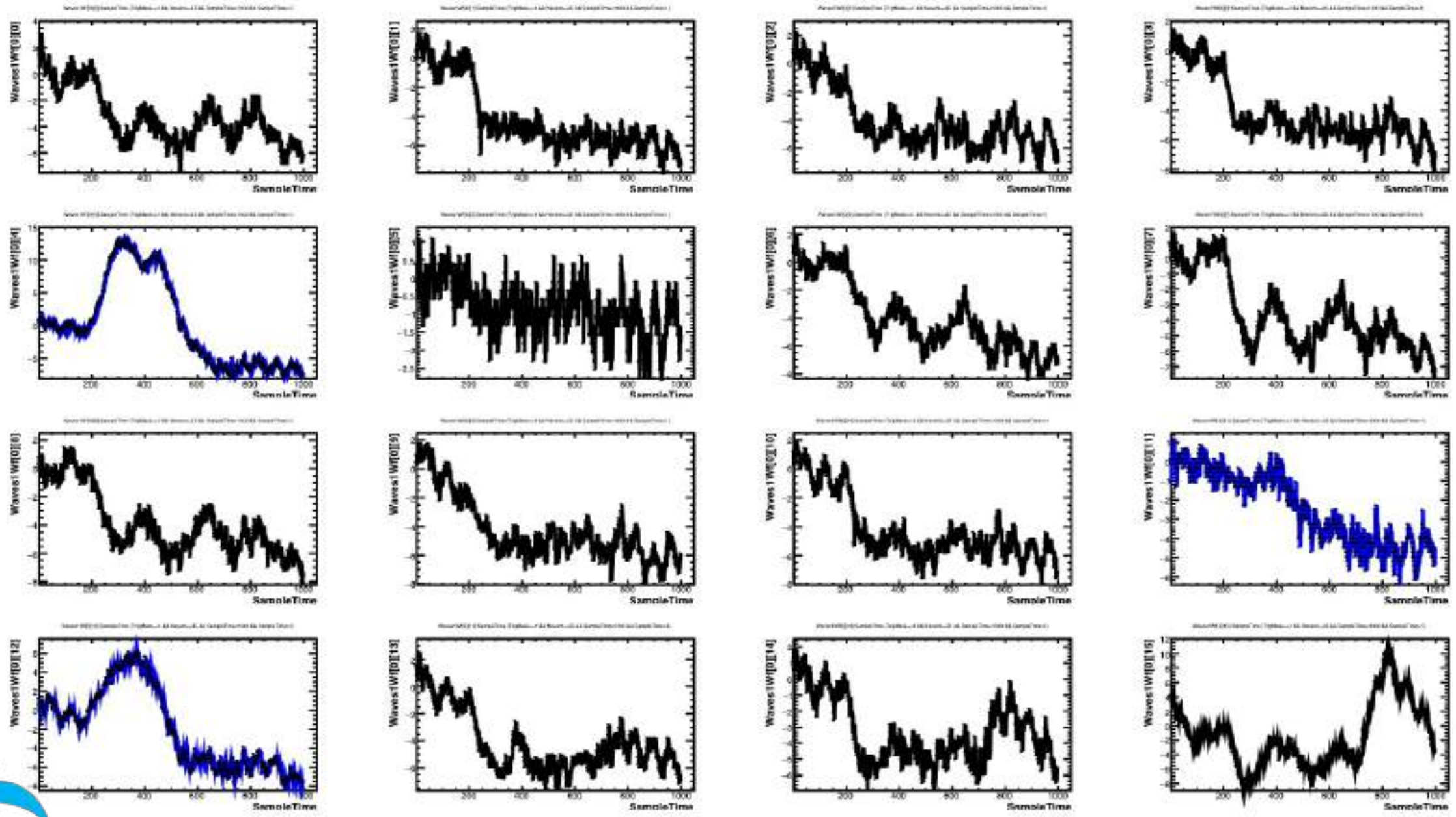

Preliminary single wf CMN subtraction

Effective beam region defined as: **7x7** area centred on the strip with the absolute maximum (X-Y)

- All other channels used to build the normalized CMN waveform
- The CMN waveform is subtracted channel-by-channel

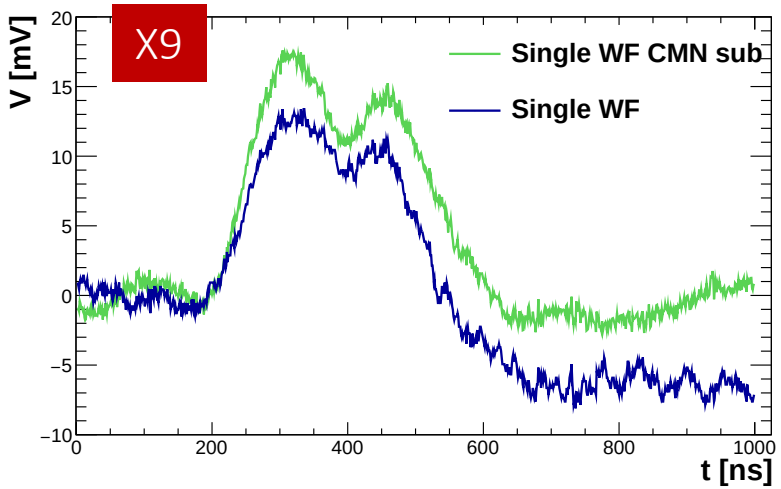

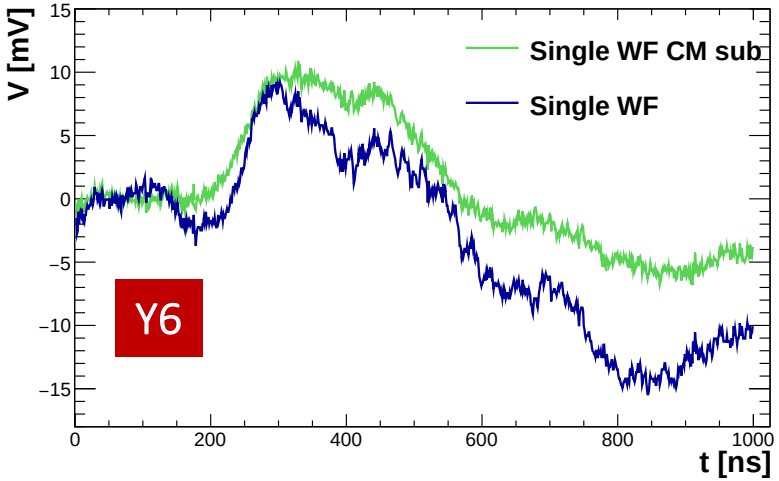

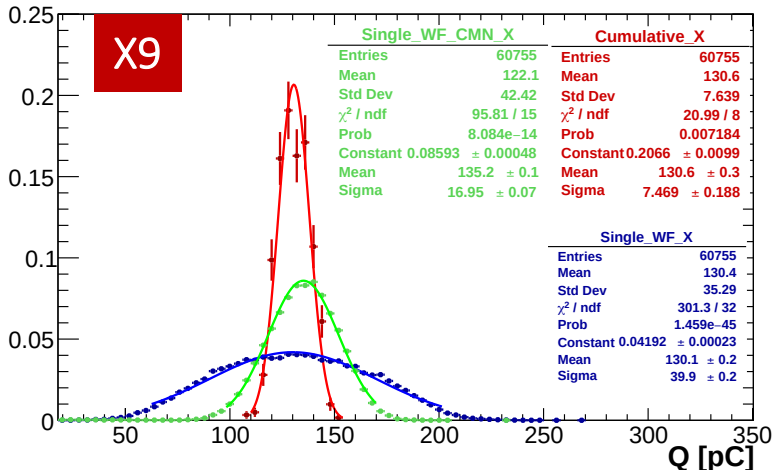

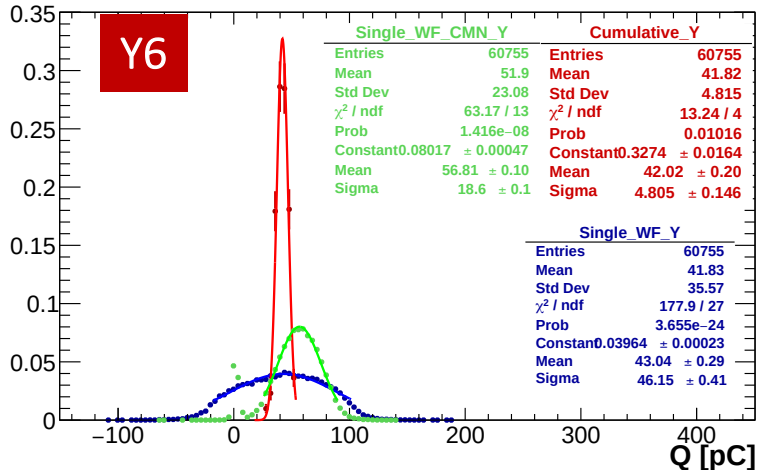

HV scan

- Beam focused @target and kept stable
- Determine the working-point
- Plateau reached @200-210 V

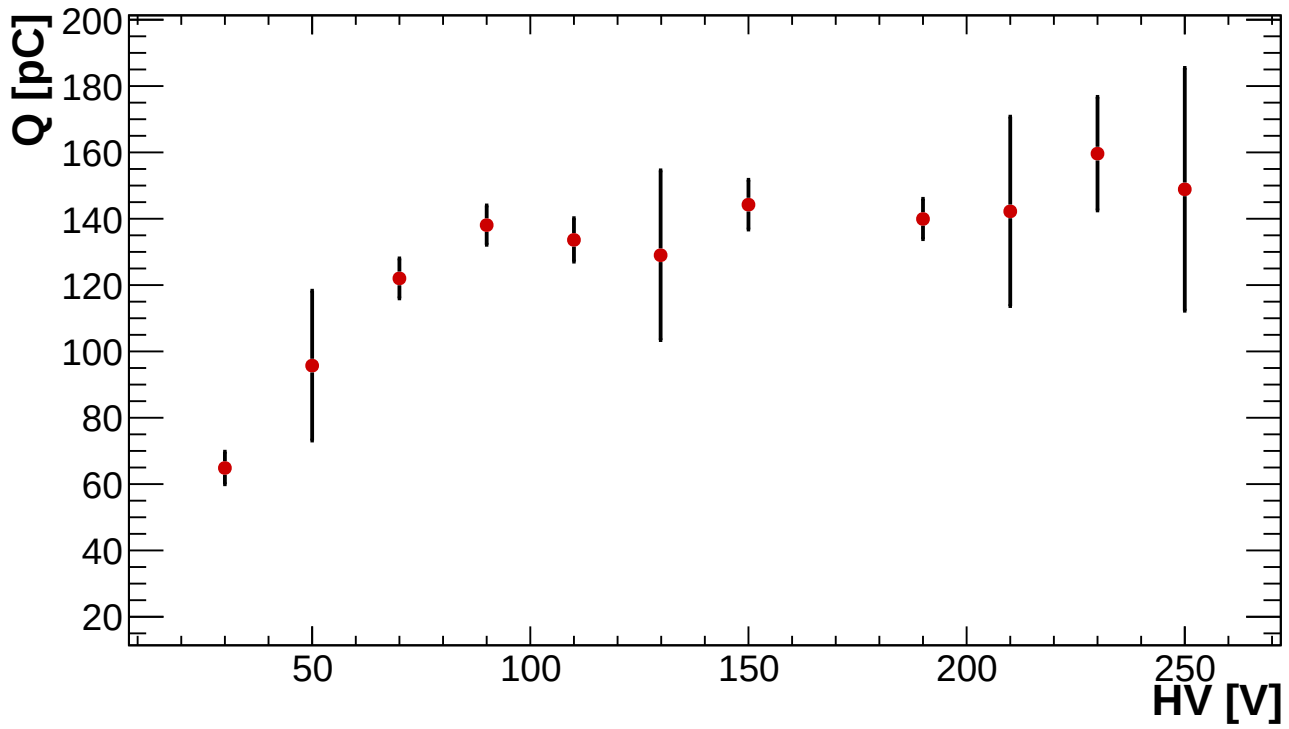

Run number	HV [V]
116	30
117	50
118	70
119	90
120	110
121	130
122	150
124	190
125	210
126	230
127	250

Radiation-induced-loss monitor

- $Q_{X\text{-}Tar}/Q_{LG}$ prompt Run III observable for the radiation-induced-loss
- $Q_{X\text{-}Tar}/Q_{LG}$ ratio per period → P0 fit to quantify loss run by run
- Some runs tested:
  - Run 344, 357, 415, 427, 472 (Scan 1) and 534, 677 (Scan 2)

→ no aging effect can be seen at this point → More data needed

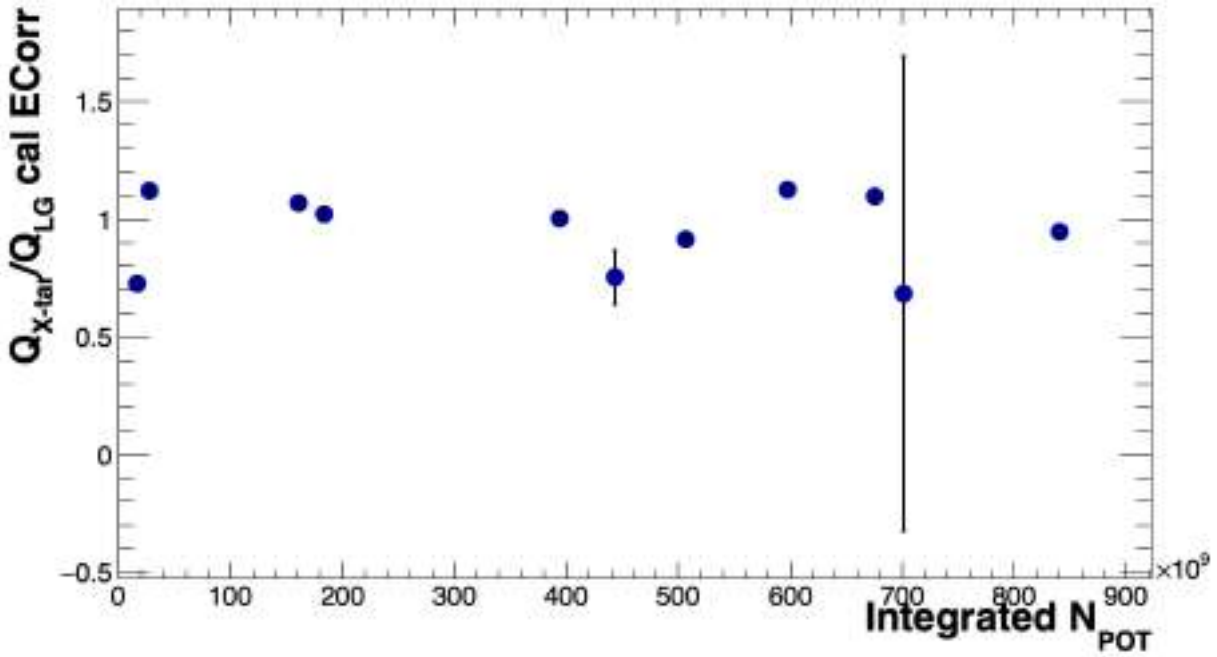

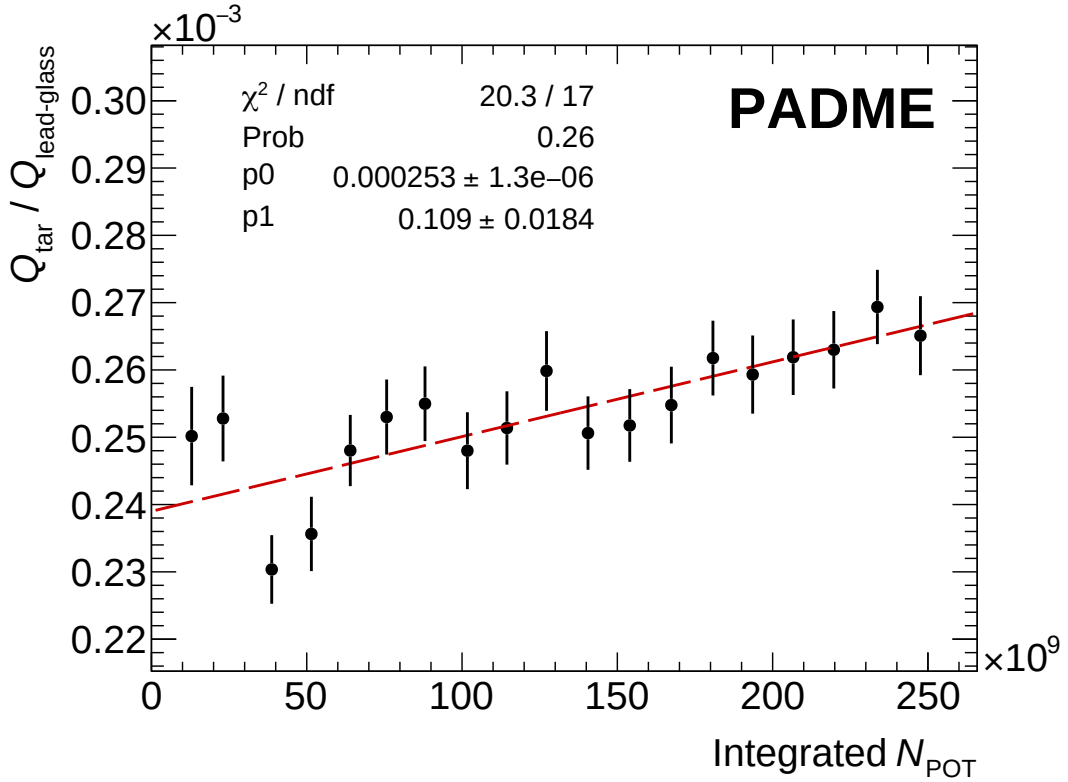

ECal - Electromagnetic Calorimeter

The main detector for the signal selection [JINST 15 (2020) T10003]:

- 616 BGO crystals, 2.1 x 2.1 x 23 cm^3
- BGO covered with diffuse reflective TiO_2 paint + 50–100 μm black tedlar foils (optical isolation)

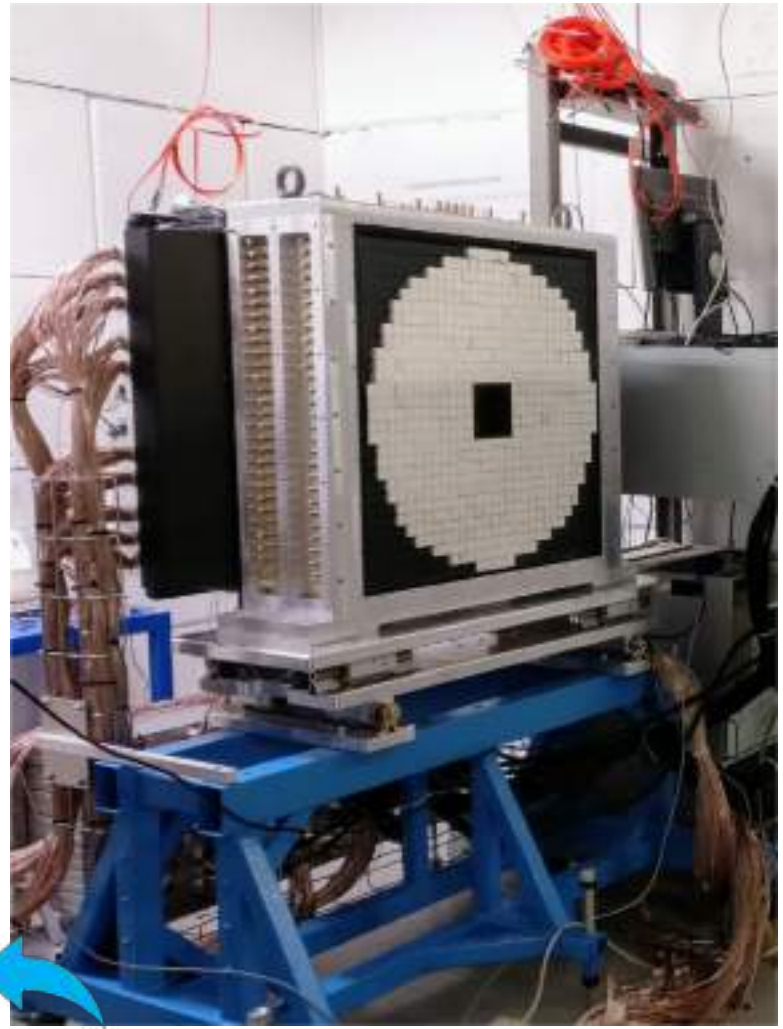

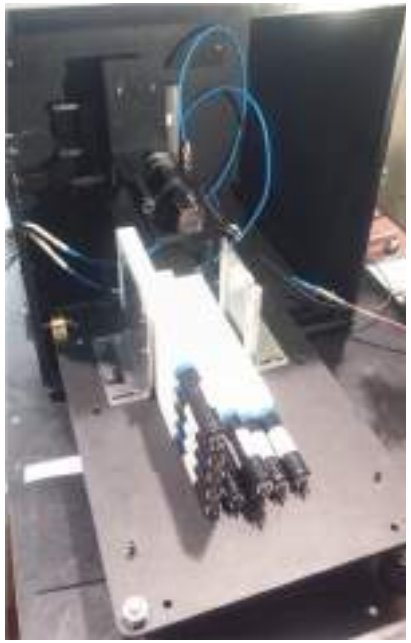

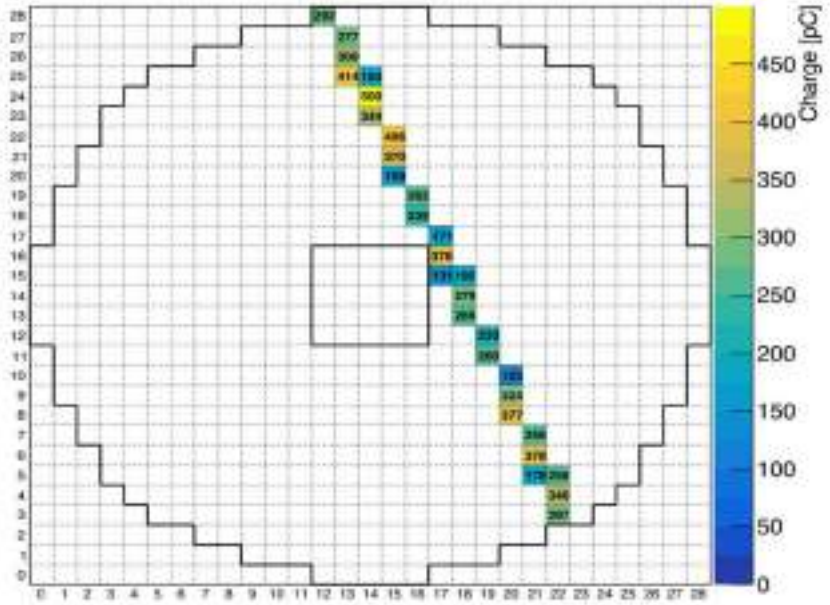

Calibration at several stages:

- BGO + PMT equalization with ^{22}Na source before construction
- Cosmic-ray calibration using the MPV of the spectrum
- Temperature monitoring + scale correction data driven

Target thickness measurement

Effective target thickness measurement → $\ell_{abs} \times \rho_C$

- Variation of the emission rate due to an absorber (PADME target and calibrated foils)
- Many sources (^{55}Fe, Cu, Rb, Mo, Ag) → X-Ray emission lines: K_α and K_β both $\mathcal{O}(5 - 25\ \mathrm{keV})$
- Quantity tested: $\nu_{obs}^{\alpha,\beta} = \nu_{true}^{\alpha,\beta} \times e^{-\sigma_{air}\Delta x_{air}} \times e^{-\sigma_{abs}\Delta x_{abs}} \times \epsilon_{acc}^{\alpha,\beta} \times \epsilon_{det}(E^{\alpha,\beta})$
- Absorption cross section σ_{abs} → *NIST*
- $\frac{\left(\nu_{obs}^{\alpha,\beta}\right)_{Abs}}{\left(\nu_{obs}^{\alpha,\beta}\right)_{noAbs}} = e^{-\sigma_{Abs}^{\alpha,\beta}\Delta x_{abs}}$ where Δx_{abs} is the absorber thickness in the proper dimension
- The final observable: $\ell_{tar} = \ln \frac{\nu_{noAbs}}{\nu_{Abs}}\Big|_{\alpha,\beta} \times \frac{A}{\rho N_A \sigma_{\alpha,\beta}}$

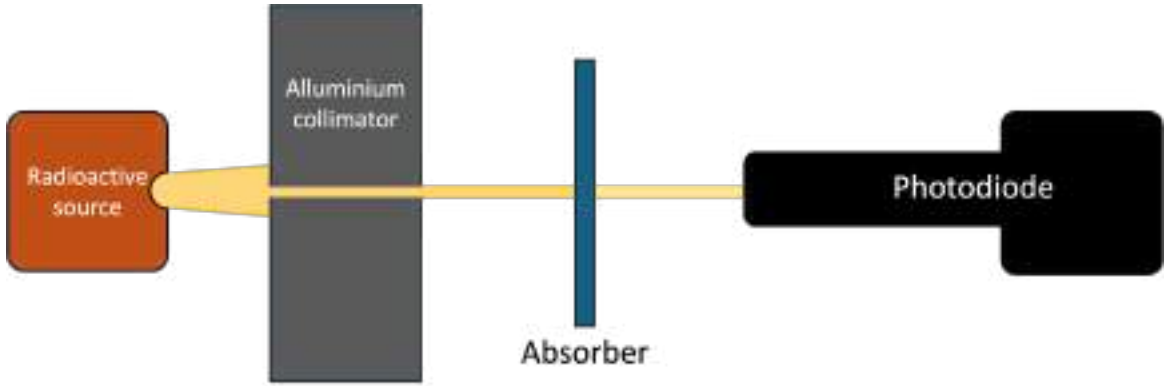

Effects to account for:

- Source identification (trade off between transparency and stopping power)
- ^{55}Fe lines diffraction in Carbon ($a_C \simeq \lambda_{\alpha,\beta}^{Fe}$)
- Compton-Rayleigh effect (order of $5 - 10\%$ depending on the absorber)
- Instability of a double logarithmic fit (proper time τ and final thickness ℓ_{tar} determination)

Diamond target thickness

Diamond target (nominally $0.1\times20\times20\ \mathrm{mm}^3, \rho = 3.515\ \frac{\mathrm{g}}{\mathrm{cm}^3}, A = 12, Z = 6$)

- Procedure validate with at **8% with certified Zn foil**
- 3 measurements performed with Cu source ($K_\alpha = 8.04\ \mathrm{keV}, K_\beta = 8.91\ \mathrm{keV}$)
- Diamond has higher transparency
  - Less stable double logarithmic fitting procedure
  - Small statistical fluctuations lead to large variation in terms of ℓ_{tar}

PADME diamond target only

Position	$\ell_{tar}(K_\alpha)$ [μm]	$\ell_{tar}(K_\beta)$ [μm]
P1	87 ± 6	120 ± 17
P2	76 ± 7	120 ± 20
P3	66 ± 5	121 ± 16

To minimise such an effect → combined target+graphitised spare measurement

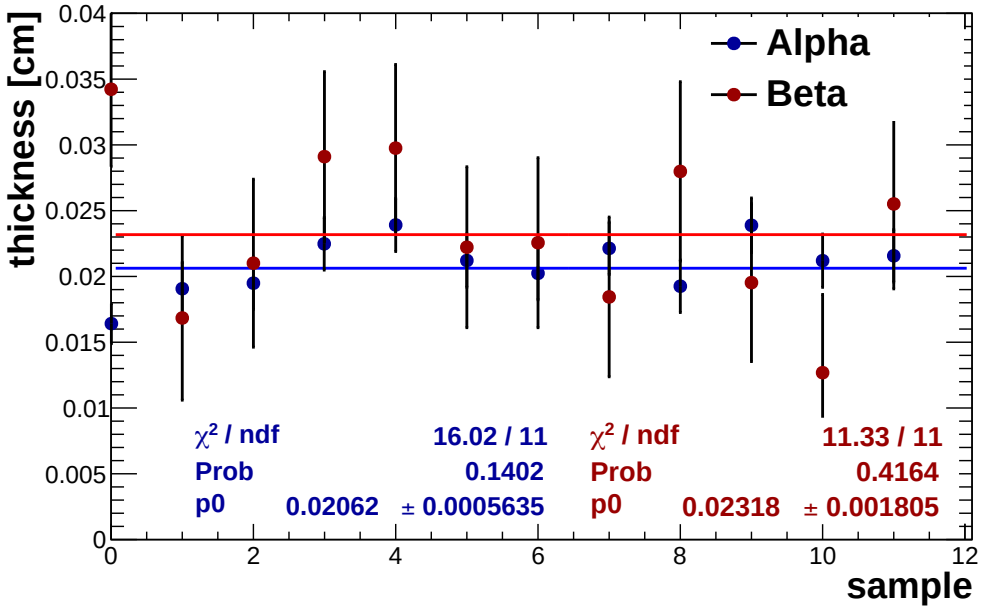

$$\ell_{tar}\big|_\alpha = \ell_{tot} - \ell_{spare} = (124 \pm 6)\ \mu\mathrm{m}$$

$$\ell_{tar}\big|_\beta = \ell_{tot} - \ell_{spare} = (149 \pm 18)\ \mu\mathrm{m}$$

Diamond target thickness - conclusion

Spare crystal effective thickness (weight)

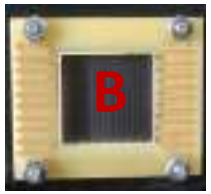

A	(0.0716 ± 0.0001) g	(50.9 ± 0.1) µm
B	(0.1155 ± 0.0001) g	(82.2 ± 0.1) µm

PADME diamond target

Position	$\ell_{tar}(K_\alpha)$ [µm]	$\ell_{tar}(K_\beta)$ [µm]
P1	87 ± 6	120 ± 17
P2	76 ± 7	120 ± 20
P3	66 ± 5	121 ± 16

Double absorber
PADME Target + Spare B

$$\ell_{tar}|_{\alpha} = (124 \pm 6)\ \mu m$$
$$\ell_{tar}|_{\beta} = (149 \pm 18)\ \mu m$$

- Single-double absorber measurements performed
  - No agreement among each other and thickness derived by weighing
  - PADME target and spare graphitised are "siblings" → no reason why they should be so much different
  - Post measurement data-quality checks performed + MC simulations for statistical treatment validation
- Two additional indirect thickness derivations:
  - On-beam multiple scattering → $\ell_{tar} = (86.8 \pm 1.5)$ µm
  - Run II Bhabha scattering → $\ell_{tar} = (88.3 \pm 0.6_{stat})$ µm
- Technique validated for Zinc-like material, while low-Z material are limited by their small attenuation for keV-photons